Control of Reproductive Floral Organ Identity Specification in *Arabidopsis* by the C Function Regulator AGAMOUS[C][W]

Diarmuid S. Ó'Maoiléidigh,[a,1] Samuel E. Wuest,[a,1,2] Liina Rae,[a] Andrea Raganelli,[a] Patrick T. Ryan,[a] Kamila Kwaśniewska,[a] Pradeep Das,[b] Amanda J. Lohan,[c] Brendan Loftus,[c] Emmanuelle Graciet,[a,3] and Frank Wellmer[a]

[a] Smurfit Institute of Genetics, Trinity College Dublin, Dublin 2, Ireland
[b] École Normale Supérieure, 69364 Lyon, cedex 07, France
[c] Conway Institute, University College Dublin, Dublin 4, Ireland

The floral organ identity factor AGAMOUS (AG) is a key regulator of *Arabidopsis thaliana* flower development, where it is involved in the formation of the reproductive floral organs as well as in the control of meristem determinacy. To obtain insights into how AG specifies organ fate, we determined the genes and processes acting downstream of this C function regulator during early flower development and distinguished between direct and indirect effects. To this end, we combined genome-wide localization studies, gene perturbation experiments, and computational analyses. Our results demonstrate that AG controls flower development to a large extent by controlling the expression of other genes with regulatory functions, which are involved in mediating a plethora of different developmental processes. One aspect of this function is the suppression of the leaf development program in emerging floral primordia. Using trichome initiation as an example, we demonstrate that AG inhibits an important aspect of leaf development through the direct control of key regulatory genes. A comparison of the gene expression programs controlled by AG and the B function regulators APETALA3 and PISTILLATA, respectively, showed that while they control many developmental processes in conjunction, they also have marked antagonistic, as well as independent activities.

INTRODUCTION

How different types of organs are formed from undifferentiated stem cells is a central question in biology. It is known that in both plants and animals, organogenesis is controlled to a large extent by master regulatory genes, which typically encode transcription factors. While it is currently not well understood how these regulators act at the molecular level, the recent development of experimental approaches that allow the characterization of protein–DNA interactions and transcriptional profiles on a genome-wide scale has led to detailed insights into the function of some of these transcription factors (Wellmer and Riechmann, 2005; Hueber and Lohmann, 2008).

In flowering plants, the different types of floral organs (i.e., sepals, petals, stamens, and carpels) are specified by the activities of a small set of master regulators, termed floral organ identity genes (Bowman et al., 1989, 1991; Coen and Meyerowitz, 1991). The pivotal role of these genes in flower development was uncovered through the identification of mutants that exhibit homeotic transformations (i.e., the replacement of one organ

type by another) (Bowman et al., 1989, 1991). Based on the phenotypes of these mutants, it was proposed that the floral organ identity genes control organ fate in a combinatorial manner (Coen and Meyerowitz, 1991). According to this so-called ABC model, sepals are specified by A function genes, petals by a combination of A and B function activities, stamens by B and C function genes, and carpels by C function gene activity alone. The molecular characterization of the genes affected in floral homeotic mutants in different species showed that they encode transcription factors and belong, with few exceptions, to the family of MADS domain transcription factors (Theissen et al., 2002). These proteins form higher-order complexes together with members of the SEPALLATA (SEP) family of transcriptional cofactors (Honma and Goto, 2001; Smaczniak et al., 2012) and preferentially bind to so-called CArG-box sequences [consensus: 5′-CC(A/T)$_6$GG-3′] (Riechmann et al., 1996a). Despite the recent genome-wide identification of the target genes of some of these transcription factors (Kaufmann et al., 2009, 2010; Wuest et al., 2012), it remains unclear how these master regulators with similar DNA binding specificities control the different developmental programs that lead to the formation of diverse organ types.

The C function gene *AGAMOUS* (*AG*) encodes a key regulator of reproductive organ development in *Arabidopsis thaliana* (Yanofsky et al., 1990). Expression of *AG* commences in incipient stamen and carpel primordia and is maintained throughout most of their development (Yanofsky et al., 1990; Drews et al., 1991). In agreement with this prolonged expression, AG is known to control several processes in addition to the specification of stamen and carpel identity. These include the control of floral meristem determinacy and patterning, microsporogenesis, and organ

maturation (Bowman et al., 1989; Ito et al., 2004, 2007). Despite the identification of several AG response and target genes in recent years (Ito et al., 2004, 2007; Gómez-Mena et al., 2005; Sun et al., 2009; Liu et al., 2011), the molecular basis underlying its activities remains largely unknown. What's more, the nature of the interplay between AG and the B function regulators and MADS domain proteins APETALA3 (AP3) and PISTILLATA (PI), which act as obligate heterodimers (Riechmann et al., 1996a; Honma and Goto, 2001; Wuest et al., 2012), is not well understood.

In this study, we identified genes and processes acting downstream of AG during the specification of reproductive floral organ identity on a global scale through a combination of gene perturbation experiments and genome-wide localization studies. Furthermore, we conducted a comparative analysis of B and C function to better understand the interplay of AG and AP3/PI during floral organ development. Our analysis also provides insights into the molecular mechanism underlying Goethe's late 18th century posit that floral organs are modified leaves (von Goethe, 1790). Using trichome formation as an example, we show that AG suppresses an important aspect of the leaf development program in part through the direct control of key regulatory genes.

RESULTS

Genome-Wide Binding Patterns of AG during Early Flower Development

To obtain insights into how C function activity leads to the specification of the reproductive floral organs, we first determined the genome-wide binding patterns of AG during early flower development. To this end, we expressed a translational fusion of AG with green fluorescent protein (AG-GFP) under the control of the regulatory regions of AG in the null mutant allele ag-1 and found that the fusion protein rescued the mutant phenotype and was expressed in the center of young floral buds in a pattern that mimics that of endogenous AG at similar developmental stages (Yanofsky et al., 1990; Drews et al., 1991) (see Supplemental Figure 1 online). We then crossed this line into a floral induction system, which allows the collection of large numbers of synchronized floral buds of early developmental stages. This system is based on the expression of a fusion protein between the floral meristem identity regulator AP1 and the hormone binding domain of the rat glucocorticoid receptor (GR) in an ap1-1 cauliflower-1 (cal-1) double mutant background (Wellmer et al., 2006). For this study, we generated an improved version of the floral induction system in which the expression of the AP1-GR fusion protein is not under control of the constitutive 35S promoter (as in the initially described line) but is driven by the regulatory regions of AP1 (including upstream and intronic sequences). Using the resulting AP1$_{PRO}$:AP1-GR AG$_{PRO}$:AG-GFP ap1-1 cal-1 ag-1 line, we induced flower development by treating plants with the steroid hormone dexamethasone and subsequently collected ~stage 5 (stages according to Smyth et al., 1990) floral buds for further analysis. We chose these flowers for our experiments because it had been reported previously that reproductive floral organ specification takes place around this stage (Ito et al., 2007), an observation we confirmed through independent experiments (see

below). Using GFP-specific antibodies, we next conducted chromatin immunoprecipitation assays coupled to next-generation sequencing (ChIP-Seq) (Figure 1) and identified 1421 high-confidence binding sites for AG-GFP in the Arabidopsis genome (see Supplemental Data Set 1 online). This number of binding sites is similar to what has been described previously for other floral organ identity factors (Kaufmann et al., 2010; Wuest et al., 2012). Binding sites were most commonly found in close proximity of transcriptional start sites, but also further upstream as well as in close proximity of the 3′ end of genes (Figure 1A). To validate the binding data, we employed several independent tests. First, an analysis of sequence motifs in the regions bound by AG revealed CArG-box-like sequences, the canonical binding sites of MADS domain proteins (Riechmann et al., 1996a), to be highly enriched (Figure 1B). Furthermore, we searched in the data set for known AG binding sites (Ito et al., 2004; Gómez-Mena et al., 2005; Sun et al., 2009; Liu et al., 2011) and found most of them to be present (Figure 1C). We also tested and confirmed selected AG binding sites in independent ChIP experiments followed by quantitative PCR analysis (Figure 1D). Lastly, we compared the genome-wide data sets obtained for AG with those previously generated for the B function regulators AP3 and PI (Wuest et al., 2012) and for the MADS domain cofactor SEP3 (Kaufmann et al., 2009). In agreement with the idea that AG can form regulatory complexes with AP3/PI and SEP3 (Riechmann et al., 1996a; Honma and Goto, 2001; Smaczniak et al., 2012), we found a high degree of correlation between the data sets for the different transcription factors (Figure 2). Taken together, the results of these analyses confirmed the validity of the ChIP-Seq data for AG.

We next compared the AG binding data to those previously described for AP1 (which is also a MADS domain protein; Mandel et al., 1992) during the initiation of flower development (Kaufmann et al., 2010) and for the floral organ identity factor AP2 (Yant et al., 2010), which belongs to the AP2/ERF family of transcription factors (Jofuku et al., 1994). While no clear correlation was found between the AG and AP2 data sets (a result that is in agreement with the idea that these transcription factors do not physically interact), the binding patterns of AG and AP1 showed a considerable overlap (Figures 2A and 2B). The latter result was surprising because AP1 and AG, in all probability, do not interact in vivo due to mutually antagonistic activities and nonoverlapping domains of expression (Yanofsky et al., 1990; Mandel et al., 1992; Gustafson-Brown et al., 1994). Furthermore, the developmental stages of the floral tissue used for the ChIP-Seq experiments for these two transcription factors were markedly different (approximately stage 5 in the case of AG; approximately stages 0 to 1 in the case of AP1). Taken together, these results suggest that the MADS domain–containing floral organ identity factors have the ability to bind to many of the same sites in the Arabidopsis genome in spite of partially nonoverlapping activities and expression patterns.

Genes Controlled Directly by AG during Early Flower Development

To identify direct AG targets, we first mapped the 1421 high-confidence binding sites we identified through ChIP-Seq to the regulatory sequences (defined as the genomic regions spanning
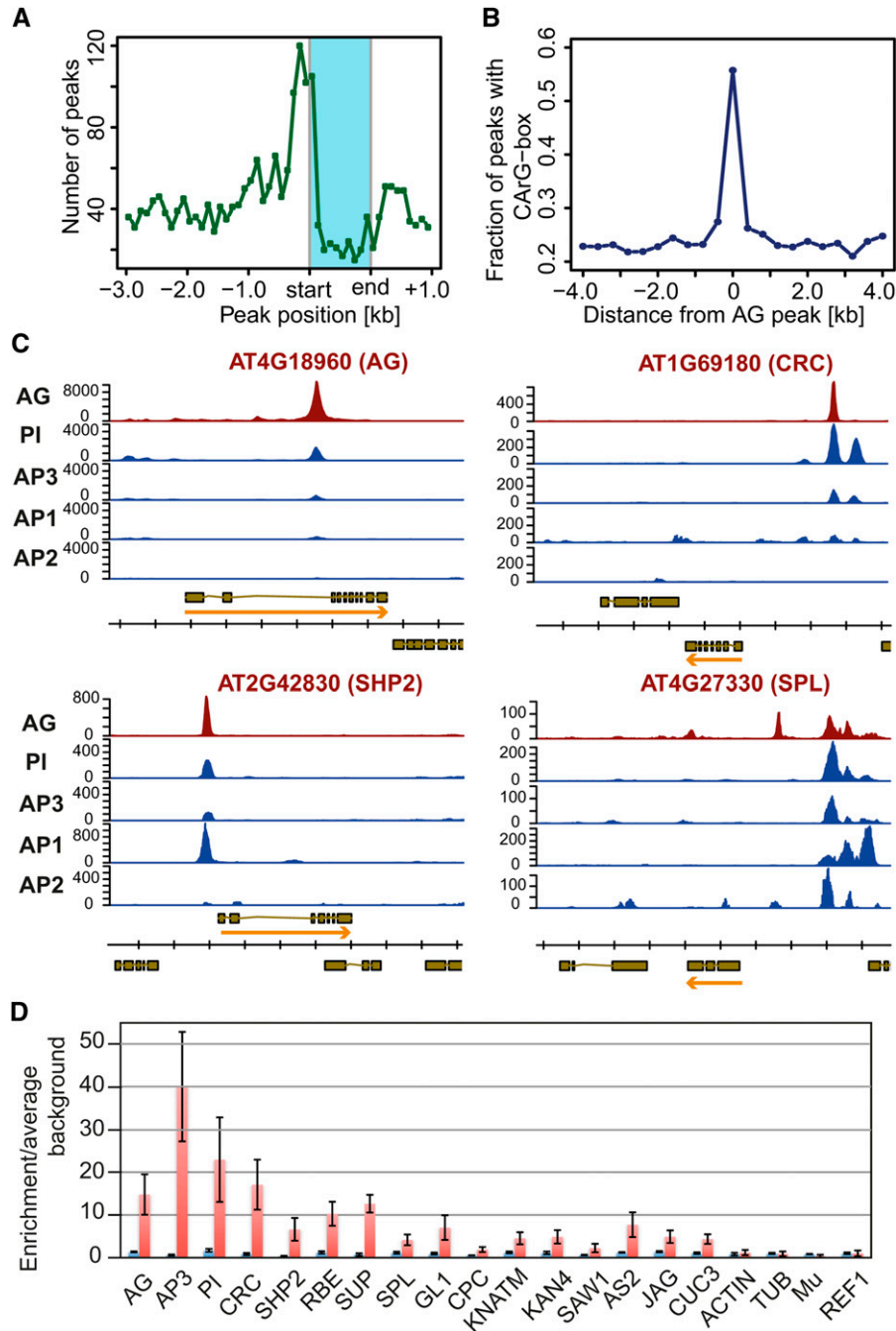
Figure 1. Global Analysis of Genomic Regions Bound by the AG Transcription Factor.

(A) Distribution of binding sites identified in the AG ChIP-Seq experiments. Plot showing the number and relative distribution of ChIP-Seq peaks in the proximity (from 3 kb upstream to 1 kb downstream) of transcribed regions. Binding site positions within transcribed regions (shaded box) were normalized relative to their length.

(B) Distribution of CArG-boxes within 400-bp windows around AG binding sites.

(C) ChIP-Seq results for selected target genes. ChIP-Seq traces for AP1 (Kaufmann et al., 2010), AP3/PI (Wuest et al., 2012), and AP2 (Yant et al., 2010) are shown for comparison. Genes found in the genomic regions analyzed, their exon-intron structures, and the direction of transcription (arrows) are indicated at the bottom of each panel. *AG*, *CRABS CLAW* (*CRC*), *SHATTERPROOF2* (*SHP2*), and *SPOROCYTELESS* (*SPL*) had been previously identified as direct AG targets (Savidge et al., 1995; Ito et al., 2004; Gómez-Mena et al., 2005).

(D) Validation of ChIP-Seq results for selected binding sites using quantitative real-time PCR. ChIP was performed using genomic DNA from inflorescence tissue of AP1$_{PRO}$:AP1-GR *ap1-1 cal-1* (blue bars) and AP1$_{PRO}$:AP1-GR AG$_{PRO}$:AG-GFP *ap1-1 cal-1 ag-1* plants (red bars), respectively,

from 3 kb upstream to 1 kb downstream of the transcribed region of a gene) of 1958 genes (see Supplemental Data Set 1 online). The number of putative AG targets is larger than that of AG binding sites because some binding sites are located within the overlapping regulatory sequences of two neighboring genes. In such cases, both genes were added to the list of putative targets.

The results of the genome-wide analyses of AP1 during floral initiation (Kaufmann et al., 2010) and of AP3/PI during early flower development (Wuest et al., 2012) implied that only a subset of the genes bound by these transcription factors are regulated by them. To identify bona fide AG targets (i.e., genes that are not only bound by the transcription factor but that also exhibit a transcriptional response to a perturbation of its activity), we compared the list of 1958 putative targets to the data of two previous studies (Ito et al., 2004; Gómez-Mena et al., 2005), in which the effects on gene expression of a specific activation of an AG-GR fusion protein in inflorescence tissue had been determined by cDNA and whole-genome microarray analysis, respectively. We found that 99 (or ~5%) of the 1958 genes that contain high-confidence AG binding sites in their putative regulatory regions were identified as differentially expressed in either of these studies (see Supplemental Figure 2 online), suggesting that AG directly controls their expression. Because this fraction was lower than what had been previously described for AP1 (~44% of genes bound by AP1 showed at least some transcriptional response; ~11% of genes exhibited robust expression changes) during floral initiation (Kaufmann et al., 2010) and for AP3/PI (~22%) during early flower development (Wuest et al., 2012), we conducted a complementary transcriptomics experiment using a loss-of-function rather than a gain-of-function approach to identify genes controlled by AG that might have been missed in the previous studies. To this end, we introduced the null mutant allele ag-1 into a floral induction system (Figures 3A and 3B) and then compared, by whole-genome microarray analysis, the gene expression profiles of mutant flowers at early developmental stages to those of corresponding flowers in which AG function was not impaired. These experiments led to the identification of 1047 genes whose expression depends, directly or indirectly, on AG activity (see Supplemental Data Set 2 online). As expected, the number of differentially expressed genes increased with progressing flower development due to the accumulative effects of AG perturbation (Figure 3F; see Supplemental Figure 2 online). To validate the microarray results, we searched for overrepresented Gene Ontology (GO) terms in the data set and found many that are associated with floral organ and floral meristem development, in agreement with AG's known functions (Figure 4A). We also identified most of the known or suspected direct AG targets among the differentially expressed genes (see Supplemental Data Set 2 online). Furthermore, we compared the microarray data set to those we

had previously generated for the B function genes AP3 and PI (Wuest et al., 2012) using a largely identical experimental approach. In agreement with the partially shared activities of these regulators and AG, we found a highly significant (P value <10^{-4}; χ^2 test; based on 283 shared genes) overlap between the differentially expressed genes identified in the two sets of experiments (see Supplemental Data Set 2 online). We also compared the microarray results to data from experiments in which gene expression in different domains of early-stage flowers had been analyzed by RNA-Seq (Jiao and Meyerowitz, 2010). We found a highly significant (P value <10^{-4}; χ^2 test; based on 324 shared genes) overlap with genes that are expressed differentially between the domains marked by AG expression (i.e., in whorls 3 and 4) and AP1 expression (i.e., in whorls 1 and 2), respectively. When we analyzed the directionality of gene expression changes in these experiments, we found that transcripts that were upregulated in ag-1 mutant flowers were overall underrepresented in the AG-expressing domain of wild-type flowers, while downregulated genes were more strongly expressed in the center of wild-type flowers when compared with the outer floral whorls (see Methods and Supplemental Data Set 2 online). Lastly, we generated a transgenic line that allows an inducible knockdown of AG activity at distinct floral stages. To this end, we first identified a functional artificial microRNA (amiRNA) (Schwab et al., 2006), which was predicted to specifically target AG (Figures 3C to 3E; see Supplemental Table 1 online), and placed it under the control of an ethanol-responsive promoter system (Roslan et al., 2001; Deveaux et al., 2003). Induction of AG-amiRNA expression resulted in a strong but reversible decrease of AG mRNA levels (Figures 3G and 3H), as well as in the transcriptional response of known or suspected AG targets (Figures 3I to 3K). We used this line to confirm the AG-dependent regulation of selected genes identified as differentially expressed in the microarray experiments (see below).

Based on the design of our microarray experiment, the differentially expressed genes we identified were predicted to be either direct AG targets or to act further downstream of the primary events (i.e., they are indirectly controlled by AG activity). To identify candidate genes that are directly regulated by AG, we compared the ChIP-Seq and microarray data and found 158 response genes that contain high-confidence binding sites in their regulatory regions. Together with the putative targets described above, we identified in total 225 unique genes that are likely under direct AG control (see Supplemental Data Set 2 online). Because the percentage of direct AG targets among the genes bound by the transcription factor was relatively small (~12%) and a comparison of large genomic data sets, such as the ones analyzed here, results inevitably in some overlap by chance, we assessed the 225 target genes with respect to their possible involvement in mediating C function. In support of the

Figure 1. (continued).

which was collected 4 d after induction of flower development. GFP-specific antibodies different from those used for ChIP-Seq were employed to ensure independence of the experiments. Data were normalized using the mean signals of four reference genomic regions: REF1 (Kaufmann et al., 2010), ACTIN, TUBULIN, and Mu transposon (Sundström et al., 2006). Bars indicate SE from the analysis of three independent biological sets of samples.
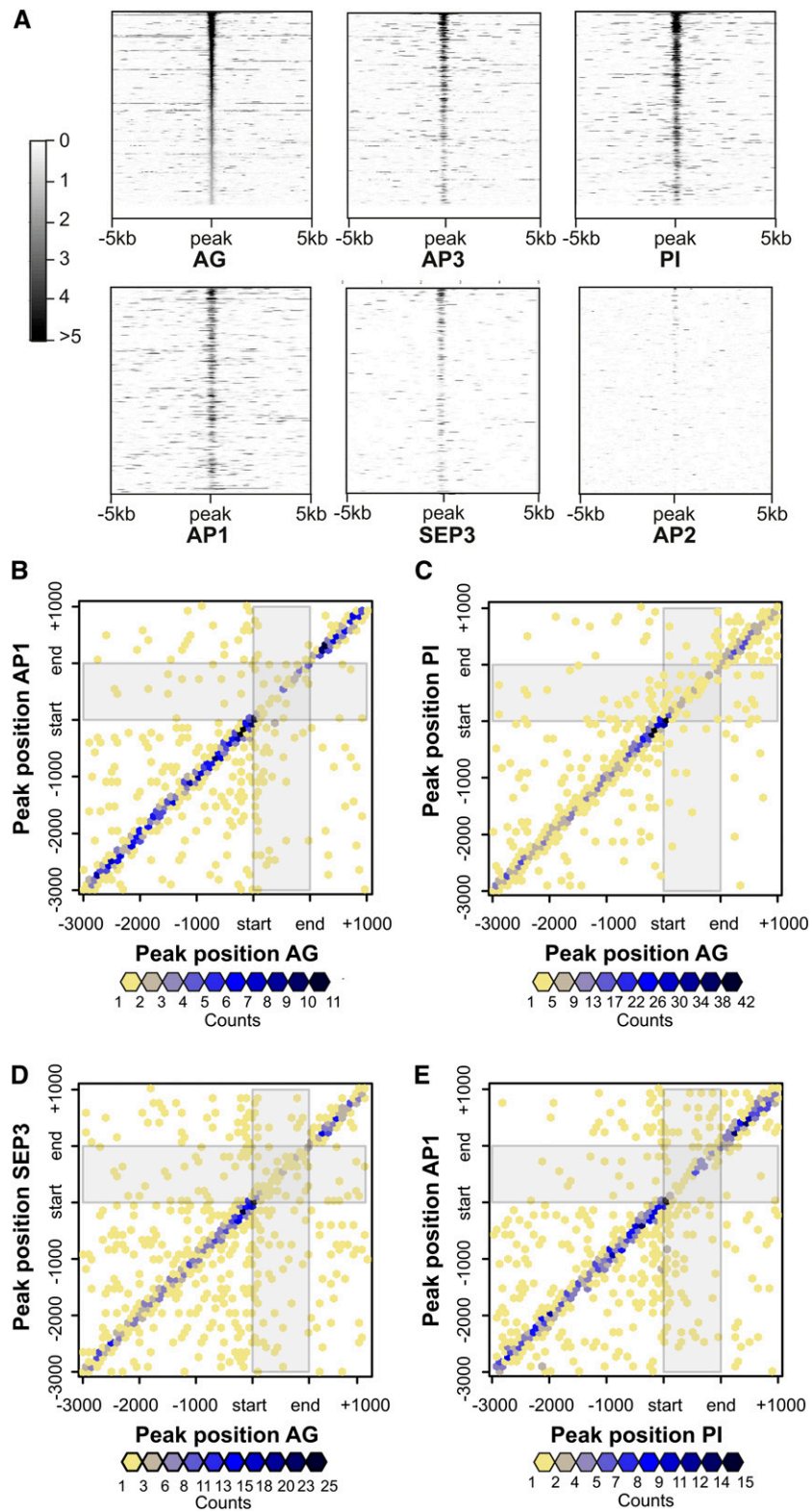
Figure 2. Comparison of Binding Data for the Floral Organ Identity Factors.

validity of our data, we found among these genes most of the known or suspected direct AG targets, including *KNUCKLES*, *CRABS CLAW*, *JAGGED*, *NOZZLE/SPOROCYTELESS*, *SHATTERPROOF2*, *SEP3*, *ARABIDOPSIS THALIANA HOMEO-BOX GENE1*, *AP1*, *AP3*, and *AG* (Gustafson-Brown et al., 1994; Savidge et al., 1995; Ito et al., 2004; Gómez-Mena et al., 2005; Sun et al., 2009). Furthermore, the list of putative AG targets contained other floral regulators known to be involved in the development of organs in whorls 3 and/or 4, such as *PI*, *SHP1*, *SUPERMAN* (*SUP*), *UNUSUAL FLORAL ORGANS*, *HECATE1* (*HEC1*), *HEC2*, and *VERDANDI* (Liljegren et al., 2000; Sakai et al., 2000; Gómez-Mena et al., 2005; Gremski et al., 2007; Matias-Hernandez et al., 2010). In fact, approximately half of the 225 direct AG target genes we identified encode proteins with regulatory functions, including many transcription factors (31% of all targets), but also (receptor) kinases, putative ligands, and proteins involved in the metabolism of and the response to different phytohormones (see Supplemental Figure 3 and Supplemental Data Set 2 online). This distribution of functional categories among the putative AG targets represents a highly significant (P value $<10^{-4}$; χ^2 test) enrichment over their genome-wide distribution (~12%), indicating that these genes were not merely selected by chance. Lastly, we used the inducible AG-amiRNA line described above and confirmed for selected targets their transcriptional dependency on AG activity (Figure 7B).

It has been suggested that some genes, which are bound by AP1 during floral initiation but that do not respond to a perturbation of its activity, might be targets at later stages of flower development when AP1 is involved in the specification of sepals and petals (Kaufmann et al., 2010). To test whether a similar scenario could explain the unresponsiveness of many genes, at early developmental stages, to binding by AG, we induced the expression of the *AG*-amiRNA in wild-type inflorescences, representing predominantly the transcriptomes of flowers of intermediate and late developmental stages (Wellmer et al., 2004). We then conducted a microarray experiment to identify genes that respond to an *AG* knockdown at advanced stages of flower formation. The 922 differentially expressed genes stemming from this experiment showed a relatively small overlap (75 genes) with the 1047 early-response genes described above, suggesting that AG controls a largely unique set of genes during later stages of flower development. We next compared the list of 922 differentially expressed genes to the 1958 genes we identified as bound by AG during early floral stages and found a significant (P value $<10^{-4}$; χ^2 test) overlap of 120 genes (see Supplemental Data Set 2 online). Seventy-five (~73%) of them

were not detected as differentially expressed at early floral stages, suggesting that these genes might be exclusively late AG targets.

Gene Expression Program Controlled by AG during Early Flower Development

The results described above showed that AG binds to many genes in the *Arabidopsis* genome, but only a relatively small fraction of them respond to a change of its activity at early stages of flower development. At the same time, we found among the high-confidence AG targets many that encode transcriptional regulators, suggesting that the widespread response on gene expression we observed after disrupting AG activity was to a large extent caused by a perturbation of these regulatory genes (i.e., as an indirect effect of AG activity). To characterize the gene expression program acting downstream of AG, we searched for overrepresented GO terms in the microarray and ChIP-Seq data separately and then calculated the reciprocal percentage of overlaps between differentially expressed genes and genes bound by AG for each term, so that the processes that are predominantly under either direct or indirect control by AG could be identified (Figure 4A). The analysis of the transcriptomics experiments done at early stages of flower development revealed that AG controls the expression of genes with known roles in a multitude of developmental processes (Figure 4A; see Supplemental Figure 3 and Supplemental Data Set 3 online). Among those, genes involved in carpel development, organ morphogenesis, regionalization, as well as in the control of meristem development and floral meristem determinacy were also strongly overrepresented in the ChIP-Seq data set, indicating that they are largely under direct regulation of AG. By contrast, genes assigned to the terms "cell cycle," "DNA repair," and "histone modification" were enriched only in the microarray data set (Figure 4A), implying that their control by AG is indirect. A closer examination of these genes showed that they are generally activated downstream of C function activity (Figure 5B). Among the genes assigned to the term "histone modification" and among genes identified through a gene family enrichment analysis (see Supplemental Figure 3 online), we identified several that encode proteins, which are predominantly involved in transposon silencing through DNA cytosine methylation, such as the chromomethylases CMT2 and CMT3, the histone methyltransferase KRYPTONITE, the chromatin remodeler DEFICIENT IN DNA METHYLATION1, and three closely related members of the ARGONAUTE (AGO) protein family (AGO4, AGO6, and AGO9) (Feng et al., 2010; Law and Jacobsen, 2010;

Figure 2. (continued).

(A) Heat maps depict the results of pairwise comparisons of binding data from different ChIP-Seq experiments (as indicated) for genomic regions surrounding 1421 AG binding sites. Normalized Poisson enrichment scores are depicted in a grayscale. All data were sorted (from top to bottom) according to descending AG peak height.
(B) to **(E)** Position of paired ChIP-Seq peaks in common target genes in the proximity of transcribed regions (3 kb upstream and 1 kb downstream) are shown for 833 common target genes of AG and AP1 (Kaufmann et al., 2010) **(B)**, 1413 common target genes of AG and PI **(C)**, 1134 common target genes of AG and SEP3 **(D)**, and 1042 common target genes of PI and AP1 **(E)**, as indicated by the color scale (counts: number of peak pairs per area unit). The frequency of binding sites (counts) in the different regions is indicated through the scale, as shown.
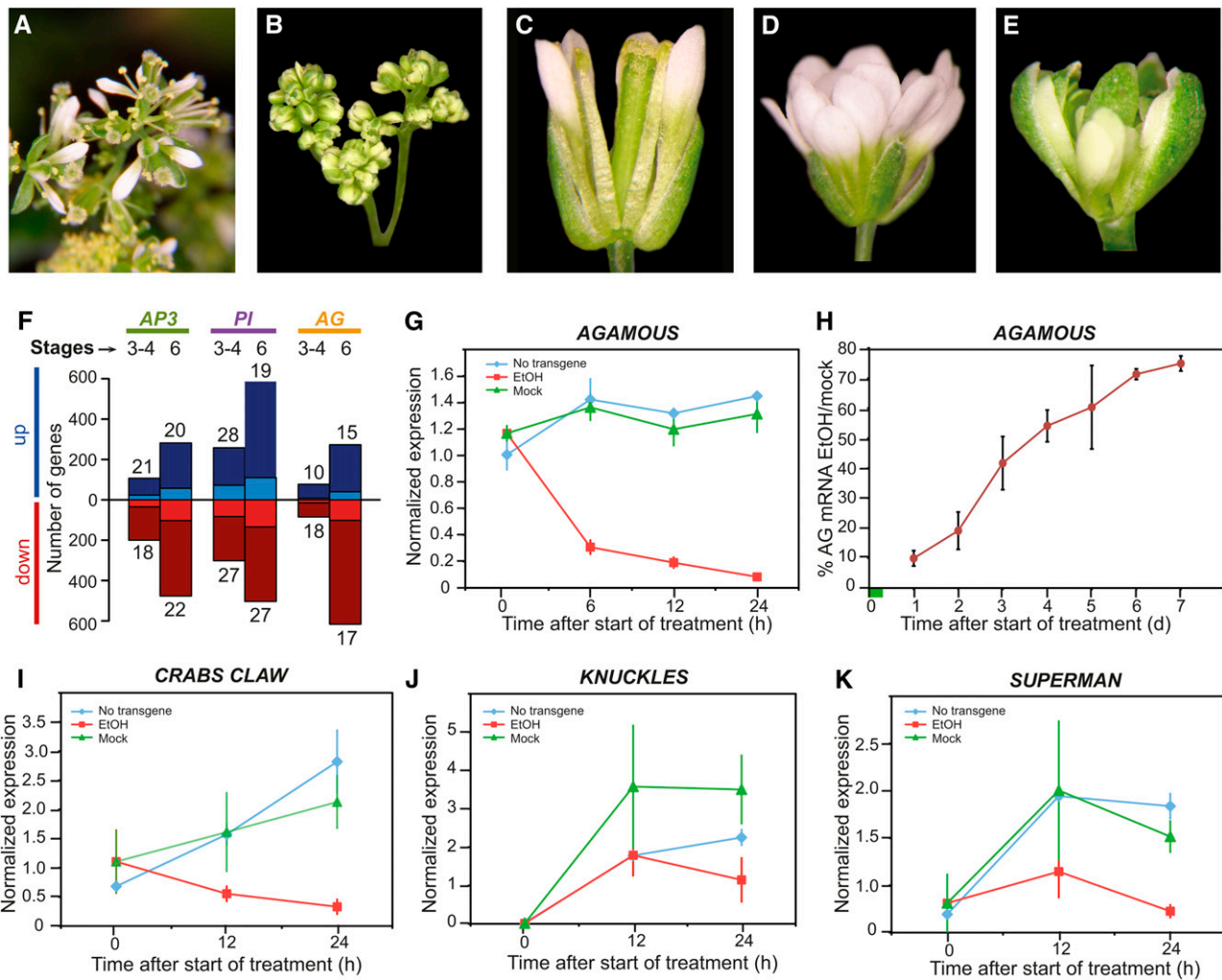[See online article for color version of this figure.]

Figure 3. Identification of AG Response Genes during Early Flower Development.

(A) and **(B)** Floral induction system based on the expression of a fusion between AP1 and the hormone binding domain of the glucocorticoid receptor in *ap1-1 cal-1* double mutant plants (Wellmer et al., 2006). Flowers produced by plants of the floral induction system with either the wild-type *AG* allele **(A)** or the strong *ag-1* mutant allele **(B)** in the background are shown. Plants were treated three times (3-d intervals in between treatments) with a dexamethasone-containing solution.

(C) to **(E)** Identification of a functional amiRNA targeting *AG*. Representative flowers from the wild type **(C)**, *ag-1* **(D)**, and 35S_{PRO}:AG-amiRNA plants **(E)** are shown.

(F) Proportion of direct targets among genes identified as up- or downregulated in the *ap3-3*, *pi-1* (Wuest et al., 2012), and *ag-1* microarray experiments (this study). Numbers above bars indicate the percentage of direct targets among differentially expressed genes. Approximate floral stages are indicated.

(G) to **(K)** Perturbation of *AG* in plants expressing an AG-amiRNA under the control of an ethanol-inducible promoter system in the background of the floral induction system. Effects on gene expression were measured by quantitative RT-PCR. Error bars indicate SE of three independent experiments.

(G) Knockdown of *AG* mRNA levels upon ethanol treatment. Plants were treated with ethanol vapor or were mock treated for different time periods (as indicated) 4 d after the induction of flower formation.

(H) Recovery of *AG* mRNA levels after an amiRNA-mediated knockdown. Plants were treated with ethanol vapor or were mock treated for 6 h (green bar); subsequently, tissue was harvested after an 18-h recovery period as well as at 24 h intervals for several days thereafter. *AG* mRNA levels in ethanol-treated plants were determined relative to those in mock-treated plants.

(I) to **(K)** Knockdown of mRNA levels of *CRC* **(I)**, *KNUCKLES* **(J)**, and *SUP* **(K)**, which are known or suspected AG targets (Sakai et al., 2000; Gómez-Mena et al., 2005; Sun et al., 2009). Plants were treated as in **(G)**. In **(G)** and **(I)** to **(K)**, mRNA levels were normalized against the mean expression of two reference genes (see Methods and Supplemental Table 3 online) in flowers of ethanol and mock-treated plants carrying the 35S_{PRO}:AlcR/AlcA_{PRO}:AG-amiRNA transgene, as well as in flowers of control plants lacking that transgene, at the 0-h time point.
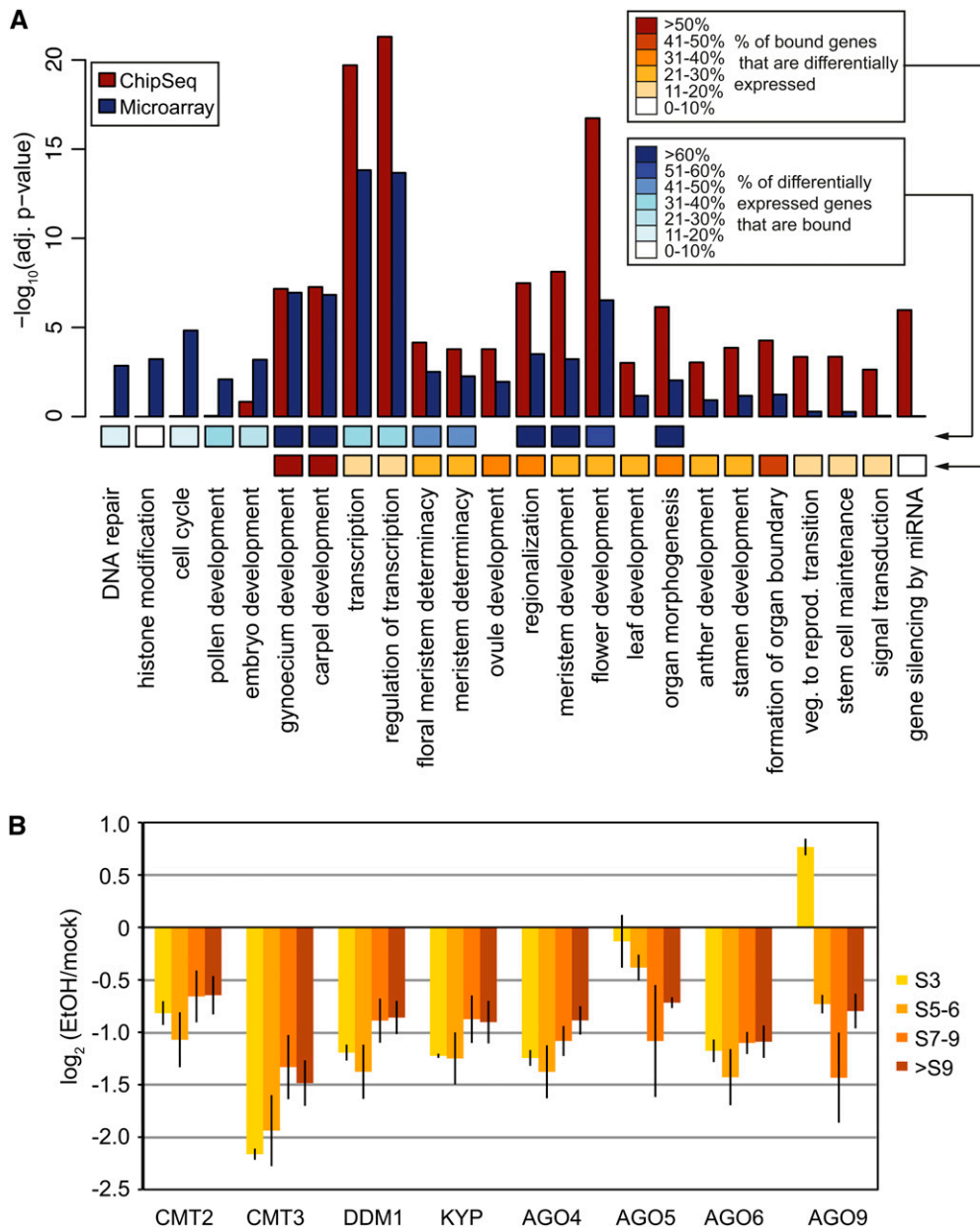
Figure 4. Processes Controlled Directly or Indirectly by AG.

(A) Selected GO terms identified as enriched in the AG ChIP-Seq data set (ChIPSeq) and among genes differentially expressed in *ag-1* mutant flowers (Microarray). Negative decadal logarithms of Benjamini and Hochberg–adjusted P values are shown. Colored boxes at the bottom of the graph indicate, for each term, the percentage of genes bound by AG that were also differentially expressed upon *AG* perturbation, as well as the percentage of differentially expressed genes that were bound by AG. A comprehensive view of GO terms is presented in Supplemental Figure 3 online.

(B) Transcriptional response of genes known or suspected to be involved in DNA cytosine methylation (see text for details) to an amiRNA-mediated perturbation of *AG* function. AP1$_{PRO}$:AP1-GR *ap1-1 cal-1* 35S$_{PRO}$:AlcR/AlcA$_{PRO}$:AG-amiRNA plants were treated with a 6-h pulse of ethanol vapor or were mock treated 1, 3, 5, and 7 d after induction of flower formation. After an 18-h recovery period, floral buds of different developmental stages (S) were collected, and mRNA levels were determined in ethanol-treated relative to mock-treated samples. Error bars indicate SE from quantitative RT-PCR experiments for three independent biological sets of samples.

Stroud et al., 2013). The results of amiRNA-mediated pertur-
bation of *AG* function at different floral stages confirmed that AG
promotes the expression of these genes throughout early flower
development (Figure 4B).

Interplay of the Gene Expression Programs Controlled by C and B Function Regulators

As described above, AG and AP3/PI have overlapping functions
in the specification of stamen primordia and can be part of the
same transcription factor complex (Riechmann et al., 1996a;
Honma and Goto, 2001; Ito et al., 2004; Wuest et al., 2012).
These transcription factors are therefore expected to share
a considerable number of target genes. In agreement with this
idea, we found a highly significant (P value $< 10^{-4}$; χ^2 test)
overlap (91 genes) between the 225 direct AG targets (see
Supplemental Data Set 2 online) and the 469 previously de-
scribed direct target genes for AP3/PI (Wuest et al., 2012). To
gain further insights into the interplay of C and B function reg-
ulators, we analyzed the gene expression programs acting both
directly or indirectly downstream of AG and AP3/PI with regard
to their differences and commonalities. To this end, we com-
pared the microarray data obtained for *ag-1* mutant flowers to
those we had previously generated for *ap3-3* and *pi-1* (Wuest
et al., 2012). We first searched for GO terms enriched in the
different transcriptomics data sets and then tested genes as-
signed to individual GO terms for coordinated directionality of
expression changes (Figure 5; see Supplemental Figure 4 on-
line). These analyses revealed a large overlap between the
processes controlled by the B and C function regulators. How-
ever, we detected both synergistic and antagonistic effects of
AP3/PI and AG activities. For example, the expression of genes
involved in stamen development is typically promoted by both
AP3/PI and AG, as expected based on their shared function
in the specification of this organ type. By contrast, genes that

mediate carpel development are often activated by AG, but re-
pressed by AP3/PI (Figure 5B). The duality of synergistic and
antagonistic activities was also observed among genes as-
signed to specific GO terms. One example includes genes in-
volved in the formation of boundaries between floral organs
(Sakai et al., 2000; Breuil-Broyer et al., 2004; Krizek et al., 2006).
SUP and *CUP-SHAPED COTYLEDON1* are positively regulated
by both AP3/PI and AG, but expression of *RABBIT EARS* is
promoted by B function and suppressed by C function activity
(see Supplemental Figure 4 online).

Our comparative analysis showed that although B and C
function regulators control many developmental processes in
conjunction, they have independent activities as well. Examples
are the genes discussed above involved in histone modification,
DNA repair, and the control of the cell cycle, which appear to be
indirectly regulated by AG without an involvement of AP3/PI
(Figure 5A). To verify this conjecture, we again focused on genes
involved in DNA methylation. We used an inducible *AP3*-amiRNA
line (Wuest et al., 2012) and tested whether these genes re-
sponded to a perturbation of B function in a similar manner as to
an *AG* knockdown (Figure 4B). We found that the expression of
most of these genes did not change significantly after induction of
AP3-amiRNA expression (see Supplemental Figure 4 online),
indicating that they are indeed predominantly under C function
control.

Suppression of the Leaf Development Program by AG

The concomitant removal of A, B, and C function activities leads
to the formation of flowers with leaf-like structures in place of
floral organs (Bowman et al., 1991). Conversely, ectopic ex-
pression of specific combinations of floral organ identity genes
causes the transformation of leaves into floral structures (Honma
and Goto, 2001; Pelaz et al., 2001). These observations strongly
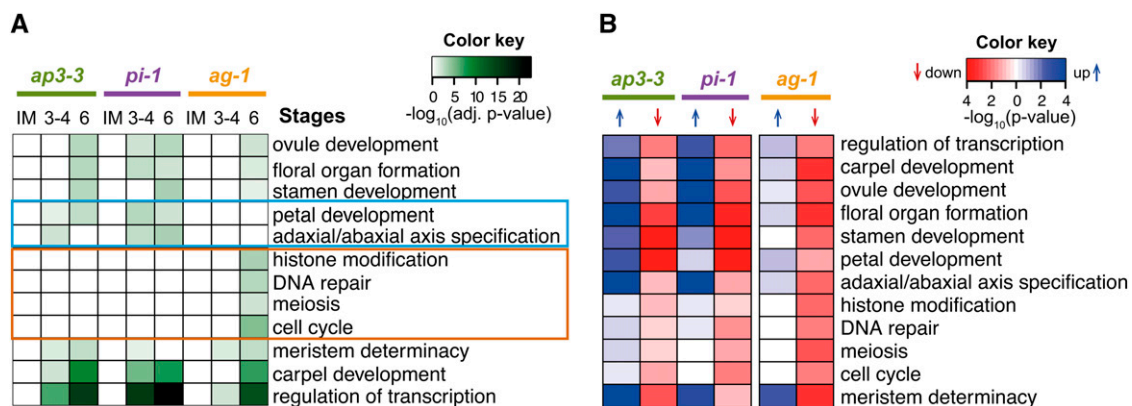support the notion that floral organs are in essence modified

Figure 5. Interplay between B and C Function Regulators.

(A) Heat map of selected GO terms overrepresented among differentially expressed genes identified in the *ap3-3*, *pi-1*, or *ag-1* microarray experiments.
Negative decadal logarithms of Benjamini and Hochberg–adjusted P values are shown. Terms specific to the *ap3-3/pi-1* and *ag-1* data sets are marked
with blue and orange boxes, respectively. A comprehensive list of significant GO terms is presented in Supplemental Data Set 3 online.
(B) Directionality of gene expression changes within selected GO terms identified in the *ap3-3*, *pi-1*, or *ag-1* microarray experiments. Negative decadal
logarithms of P values are shown for a test for coordinated up- or downregulation (as indicated). A comprehensive list of significant GO terms is presented in
Supplemental Figure 4 online and Supplemental Data Set 3 online.

leaves and that the floral organ identity factors are necessary and sufficient for converting leaves into floral organs. However, the molecular mechanisms underlying this transformation process are largely unknown. One possibility is that the floral organ identity factors activate a new developmental pathway (that of the flower), which then simply overrides the underlying leaf program. Alternatively, they could, directly or indirectly, modulate or suppress the activities of key regulators of leaf development, in addition to the activation of genes needed specifically for the formation of floral organs (Sablowski, 2010). To gain insights into the mechanism underlying the reprogramming of leaves during floral organ formation, we first queried an *Arabidopsis* gene expression atlas consisting of 65 different tissues and cell types (see Methods and Supplemental Data Set 4 online for details) with the genes we had identified as differentially expressed in young *ag* mutant flowers (Figure 6). In agreement with the role of C function activity in the specification of the reproductive floral organs, we found that genes with high expression in gametophytic tissues were overrepresented among genes activated by AG (Figure 6B). By contrast, genes repressed by AG were strongly enriched for transcripts with highest expression in leaves (Figure 6B). A closer examination of the leaf-associated transcripts

revealed that many of them encode proteins with known roles in photosynthesis and that the corresponding genes are often indirectly controlled by AG (see Supplemental Data Set 4 online). Thus, genes with predominant expression in leaves were derepressed in young *ag* mutant flowers, suggesting that the suppression of the leaf developmental program occurs at early floral stages. In agreement with this idea, we observed a similar enrichment of leaf-associated transcripts among genes repressed by AP3/PI during early flower development (Figure 6C).

Because we found regulators of leaf growth, polarity, and differentiation among the genes targeted by AG during floral organ identity specification (Figure 4A; see Supplemental Data Set 2 online), we hypothesized that AG may mediate the suppression of leaf development at least in part through direct interactions with the regulatory regions of these genes. To test this, we focused on several regulators of trichome initiation, which included the activators *GLABRA1* (*GL1*) and *ZINC-FINGER PROTEIN8* (*ZFP8*) (Larkin et al., 1994; Gan et al., 2007), as well as the repressors *TRICHOMELESS1* (*TCL1*), *CAPRICE* (*CPC*), and *CYTOKININ OXIDASE/DEHYDROGENASE6* (*CKX6*) (Schellmann et al., 2002; Wang et al., 2007; Steiner et al., 2012). *GL1*, *CPC*, and *CKX6* contain AG binding sites in their putative regulatory
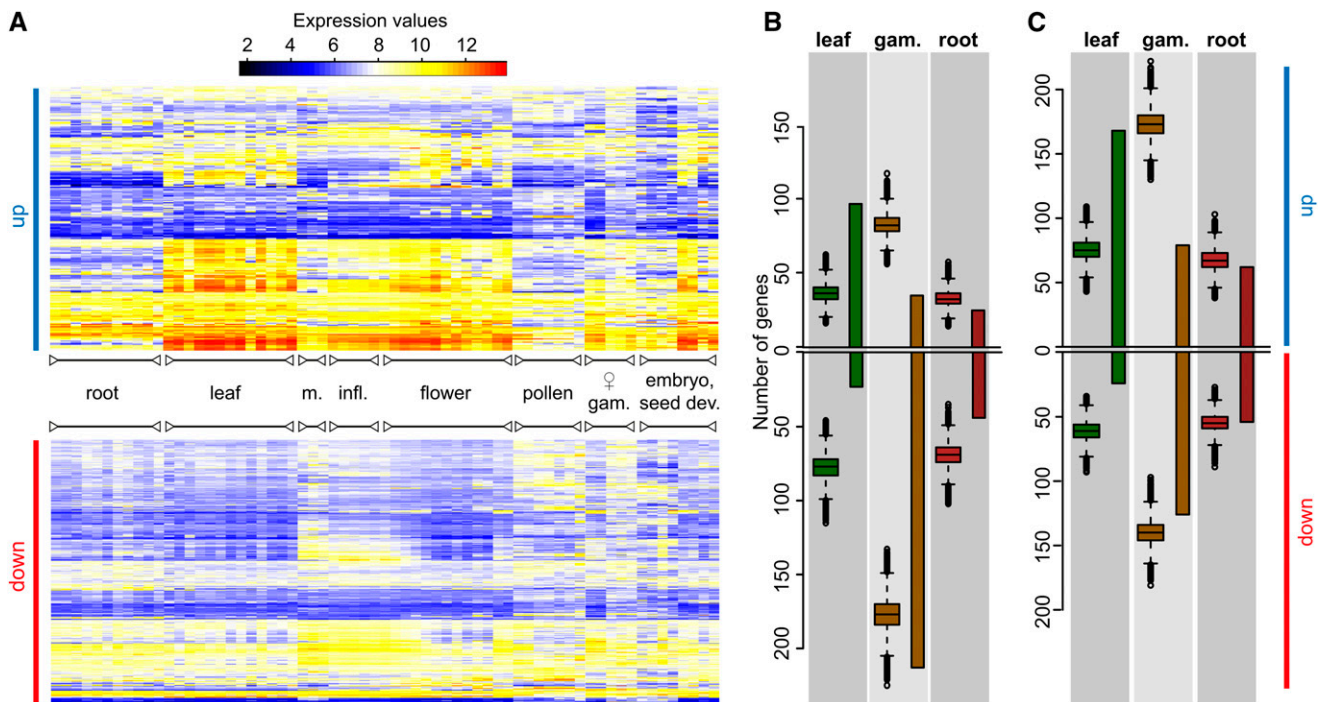

Figure 6. Global Expression Patterns of Genes Controlled by B and C Function Regulators.

(A) Expression of genes identified as up- (top) or downregulated (bottom) in the *ag-1* microarray experiments across 65 different *Arabidopsis* tissue samples (see Methods for details). Transcriptomics data sets from the analysis of individual tissue samples were grouped into eight categories: root, leaf, meristem (m.), inflorescence (infl.), flower, pollen, female gametophyte (♀ gam.), and embryo and seed development. Expression values are indicated through a color-coded scale.

(B) and **(C)** Numbers of genes identified as up- (top) or down-regulated (bottom) in the *ag-1* **(B)** and *pi-1* **(C)** microarray experiments that showed peak expression in either leaves, gametophytic tissues (gam.), or roots are indicated through colored bars. To test for significant enrichment of these genes in the data sets, 100,000 equally sized sets of randomly selected *Arabidopsis* genes were likewise analyzed, and results are shown through box-and-whisker plots.

regions (Figure 7A) and thus are likely direct AG targets, while *ZFP8* and *TCL1* are, in all probability, under indirect control. We used the inducible amiRNA line for *AG* to determine the effects of a knockdown of AG activity on the expression of these genes. We found that upon *AG* perturbation, the transcript levels of *GL1* and *ZFP8* were increased and those of *TCL1*, *CPC*, and *CKX6* were reduced (Figure 7B). Thus, AG normally downregulates the expression of activators of trichome initiation and promotes that of the repressors. We therefore tested whether the AG-dependent transcriptional control of these genes might lead to an inhibition of trichome initiation on reproductive floral organs, which are typically trichomeless. To this end, we used the inducible amiRNA line for *AG* described above and assessed floral phenotypes at time of anthesis (stage 13) after a pulsed knockdown of C function activity in whole inflorescences. Largely in agreement with the results of a previous study (Ito et al., 2007), we found that AG has distinct functions during the course of flower formation, as indicated by the appearance of different floral phenotypes depending on the developmental stage at which *AG* activity was perturbed (Figure 8). Flowers in which the induction of amiRNA expression had occurred during late stages (10 to 13) formed aberrantly shaped carpels, as well as stamens and (surprisingly) petals, which were both underdeveloped. By contrast, homeotic transformations of stamens and carpels and the formation

of extra floral whorls (i.e., the characteristic features of strong *ag* mutant alleles) were observed in flowers treated at early developmental stages (3 to 6) with several ethanol pulses (Figure 8N). Notably, in flowers in which *AG* had been knocked down at intermediate stages, we observed the formation of trichomes on carpel valves (Figures 9A to 9F), in agreement with the observed misexpression of regulators of trichome initiation. Most of these trichomes were branched (see Supplemental Figure 5 online), which is a hallmark of trichomes on leaves compared with those on sepals, which are typically unbranched (Bowman et al., 1989; Ditta et al., 2004). In agreement with the idea that the observed transformations led to leaf-like rather than sepal-like tissue, we found that the morphology and cell patterns of the carpel valves that bore trichomes were similar to those of leaf surfaces (Figures 9G and 9H) but did not resemble those of sepals (Figure 9I) or the bract-like first-whorl organs of *ap1-1* mutant flowers (Figure 9J).

To further investigate the link between C function and trichome initiation, we tested, using a previously published 35S$_{PRO}$:AG-GR line (Ito et al., 2004), whether AG could suppress trichome formation in leaves. We found that an ectopic activation of the AG-GR fusion protein did not lead to any discernable changes in trichome patterns when compared with control plants (see Supplemental Figure 5 online), suggesting that additional
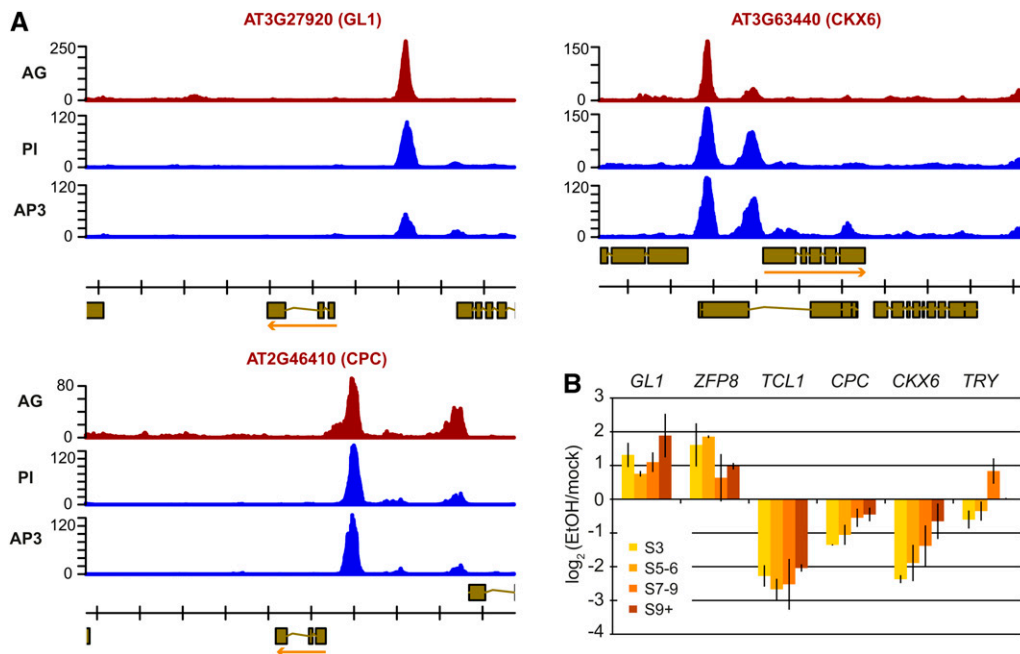

Figure 7. Transcriptional Control of Regulators of Trichome Initiation by AG.

(A) AG, PI, and AP3 ChIP-Seq results for *GL1*, *CKX6*, and *CPC*. Genes found in the genomic regions analyzed, their exon-intron structures, and the direction of transcription (arrows) are indicated at the bottom of each panel.

(B) Transcriptional response of genes involved in the control of trichome initiation (see text for details) to amiRNA-mediated perturbations of *AG* function. Plants carrying 35S$_{PRO}$:AlcR/AlcA$_{PRO}$:AG-amiRNA transgenes in the background of the floral induction system were treated with a 6-h pulse of ethanol vapor or were mock treated 1, 3, 5, and 7 d after induction of flower formation. After an 18-h recovery period, floral buds of different developmental stages (S) were collected, and mRNA levels were determined in ethanol-treated relative to mock-treated samples. Bars indicate SE from quantitative RT-PCR experiments for three independent sets of samples.

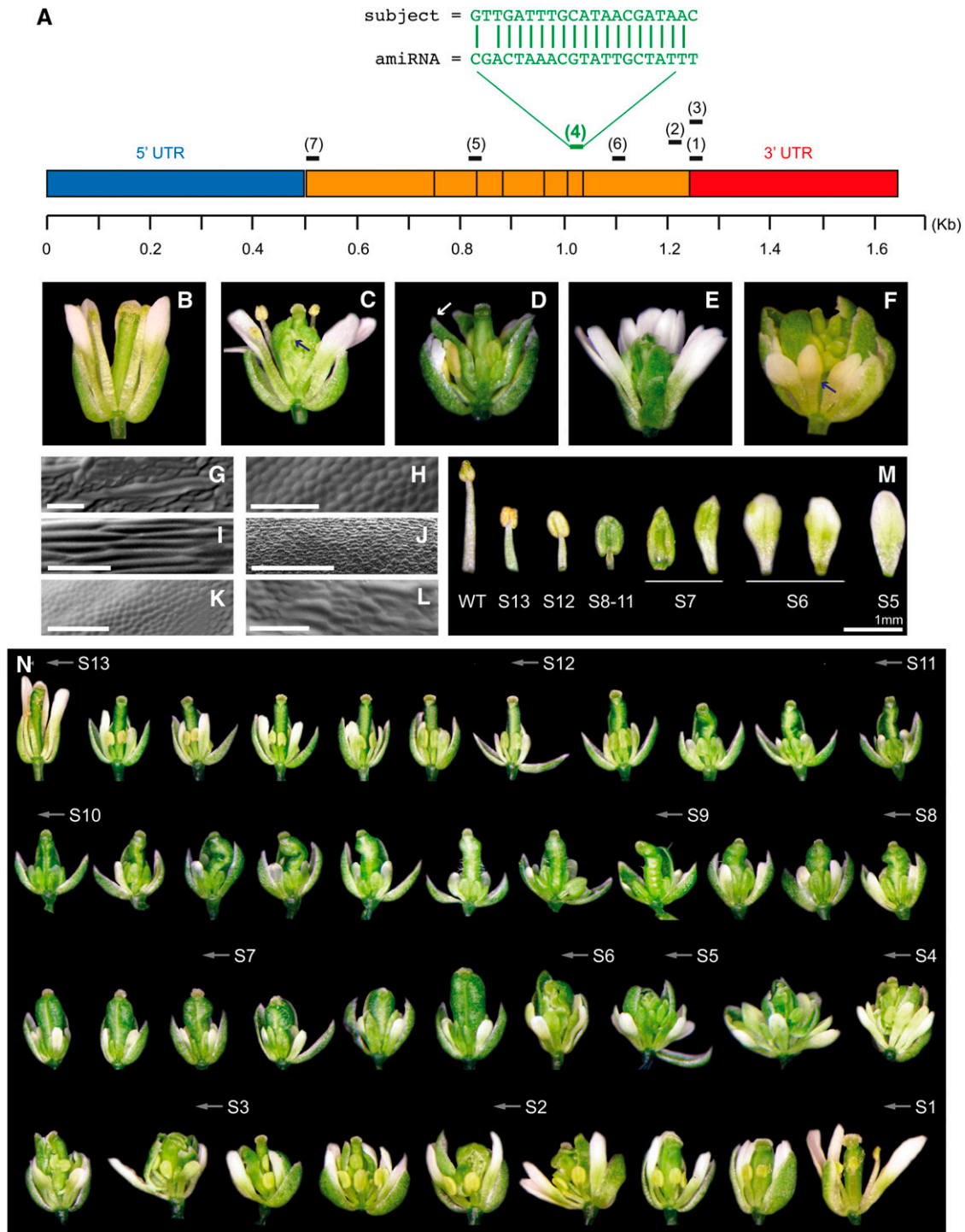[See online article for color version of this figure.]

Figure 8. Morphological Effects of a Pulsed Perturbation of AG Activity.

(A) Schematic representations of the *AG* cDNA, including exon boundaries. The target sites of seven different amiRNAs tested (see Supplemental Table 1 online) are shown. The sequence of the amiRNA (noted AG4-amiRNA) whose overexpression led to an *ag* mutant phenotype and its target sequence are indicated. UTR, untranslated region.

(B) A wild-type flower (one first whorl sepal was removed).

(C) to **(F)** Flowers of 35S$_{PRO}$:AlcR/AlcA$_{PRO}$:AG-amiRNA plants treated with one 6-h pulse of ethanol vapor (one first whorl sepal removed) **(C)**, two 6-h pulses of ethanol vapor (with a 42-h recovery period in between treatments; one first whorl sepal removed) **(D)**, five 6-h pulses of ethanol vapor (with

flower-specific regulators are required to mediate the AG-dependent suppression of trichome initiation.

We next tested whether the appearance of trichomes on carpels after an amiRNA-mediated perturbation of *AG* activity depended on the identity of the affected organ or on its position in the center of the flower. To this end, we induced the expression of the *AG*-amiRNA in inflorescences of *ap2-2* mutant plants, whose flowers are characterized by the transformation of sepals into carpels (Figure 10A) as a result of the expansion of the *AG* expression domain into the outer floral whorls (Drews et al., 1991). We observed the formation of trichomes on the first-whorl carpelloid organs of *ap2-2* flowers (Figure 10B), in which AG activity had been perturbed at intermediate stages, suggesting that the effect of AG on trichome initiation is not whorl specific. These flowers had also extra floral whorls but did not exhibit the homeotic organ transformations typically observed after a loss of C function, suggesting that the activities of AG in the control of floral meristem determinancy and floral organ specification can be temporally separated (Figure 8N).

Interplay of B and C Function Regulators in the Suppression of Trichome Formation

The amiRNA-dependent knockdown of AG activity in wild-type inflorescences led to the formation of trichomes on carpels, but not on stamens, despite the fact that *AG* is also expressed in this organ type (Yanofsky et al., 1990; Drews et al., 1991). Because our ChIP-Seq data for AP3 and PI (Wuest et al., 2012) showed that these transcription factors can also bind to the regulators of trichome formation targeted by AG (Figure 7A), we

hypothesized that the lack of trichome formation on stamens in the absence of C function may be due to B function activity. However, amiRNA-mediated knockdowns of *AP3* and *PI* at different stages of flower development did not result in abnormal trichome patterns (Wuest et al., 2012). Furthermore, when we used an ethanol-inducible amiRNA line for *AP3* (Wuest et al., 2012) and measured, at different stages of flower development, the expression levels of the regulators of trichome initiation controlled by AG after a perturbation of *AP3* activity, we found that their expression levels were (with the exception of *GL1*) not as consistently affected as in the case of an *AG* knockdown (see Supplemental Figure 5 online). We therefore considered the possibility that B and C function regulators might act redundantly in the control of trichome initiation. To test this, we combined inducible amiRNA lines against *AG* and *PI* and then induced the expression of both amiRNAs in inflorescences to simultaneously knock down B and C function activities. In agreement with the idea that the B and C function regulators control trichome initiation in a redundant manner, anthers of flowers, which formed after the induction of amiRNA expression, occasionally carried one or two branched trichomes (Figure 10D). This phenotype (and its relatively low penetrance) is reminiscent of plants overexpressing *GL1* in a mutant background, in which *TRIPTYCHON* (*TRY*), a key repressor of trichome initiation, is nonfunctional (Schnittger et al., 1998). In contrast with the observed effect on stamens, trichome formation on carpels was unaltered in these plants compared with an induction of the *AG*-amiRNA alone (Figure 10C), a result that can be readily explained by the absence of B function in the center of the flower (Jack et al., 1992; Goto and Meyerowitz, 1994).

Figure 8. (continued).

a 42-h recovery period in between treatments; one first whorl sepal removed) **(E)**, and five 6-h pulses of ethanol vapor (with a 66-h recovery period in between treatments; one first whorl sepal was removed) **(F)**. These timed inactivation experiments showed that the requirement for *AG* activity differs for different processes regulated by AG. While termination of the floral meristem was already delayed after a single pulse of ethanol vapor **(C)**, a prolonged perturbation of AG function was required to completely abolish stamen identity in the third whorl (**[E]** and **[F]**). Arrows in **(C)** and **(F)** point to stigmatic tissue on 4th whorl sepal-like organs **(C)** and to a third whorl stamen, which is only partially transformed into a petal **(F)**.
(G) to **(J)** Abaxial epidermal surface images of different floral organs. Cell morphology of a first whorl sepal **(G)**, a second whorl petal **(H)**, a third whorl stamen filament **(I)**, and a fourth whorl carpel valve of a wild-type flower **(J)**.
(K) Cell morphology of a third whorl organ of a $35S_{PRO}$:AlcR/AlcA$_{PRO}$:AG-amiRNA flower treated with five pulses of 6 h of ethanol vapor (with a 42-h recovery between treatments). Note the similarity in cell morphology with a wild-type petal.
(L) Cell morphology of a fourth whorl organ of a $35S_{PRO}$:AlcR/AlcA$_{PRO}$:AG-amiRNA flower treated with one pulse of 6 h of ethanol vapor. The cell morphology is similar to that found in sepals. Bars = 200 μm.
(M) The gradual transformation of third whorl stamens into petals upon amiRNA-mediated perturbation of *AG* activity at different stages of flower development. $35S_{PRO}$:AlcR/AlcA$_{PRO}$:AG-amiRNA plants were treated with five 3-h pulses of ethanol vapor with a 42-h recovery period in between treatments. Third whorl organs were photographed at time of anthesis (stage 13). The approximate stage (S) of flower development at which the *AG* knockdown commenced is indicated at the bottom. WT, the wild type. Bar = 1 mm.
(N) Phenotypic effects of *AG* perturbation at different stages of flower development. $35S_{PRO}$:AlcR/AlcA$_{PRO}$:AG-amiRNA plants were treated with five 3-h pulses of ethanol vapor with a 42-h recovery period in between treatments. Flowers were photographed at time of anthesis (stage 13). Approximate floral stages at the time of *AG* perturbation are indicated (labels mark the beginning of each stage). When *AG* activity was disrupted at late stages of flower development (10-13), flowers with misshapen gynoecia and reduced stamen and petals were observed, suggesting that *AG* is required for organ growth. Flowers in which *AG* activity had been disrupted during intermediate stages (~8 to 9) of flower development exhibited small green stamens and trichomes on carpel valves (see also Figure 9). Perturbation of *AG* function in approximately stage 5-6 flowers resulted in the transformation of stamens and carpels into petals and sepals, respectively, while a loss of floral meristem determinancy was observed in flowers in which *AG* activity was disrupted at early stages (3-4).
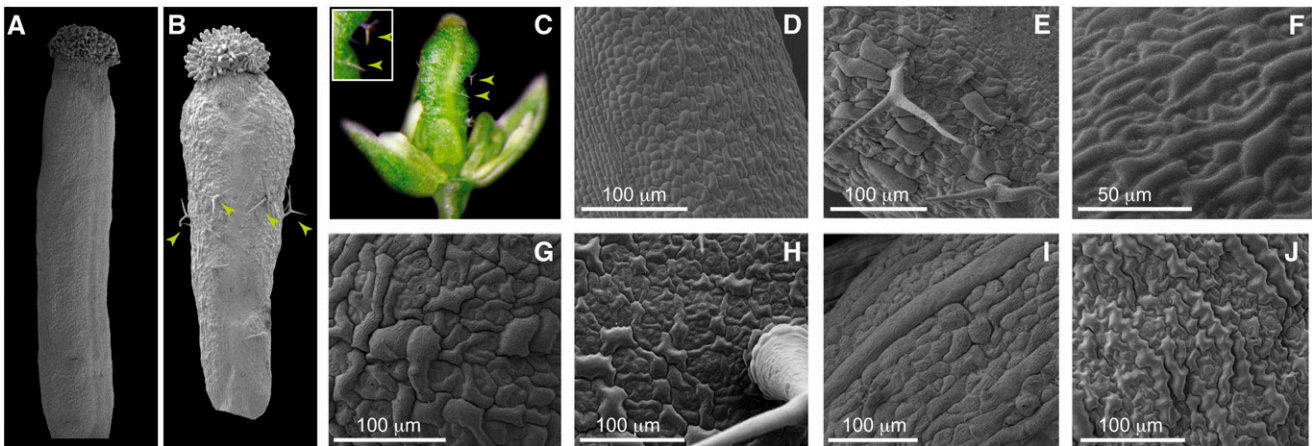[See online article for color version of this figure.]

Figure 9. Knockdown of *AG* Activity Leads to the Formation of Trichomes on Carpel Valves.

(A) and **(B)** Scanning electron micrographs of gynoecia from untreated **(A)** and ethanol-treated **(B)** 35S$_{PRO}$:AlcR/AlcA$_{PRO}$:AG-amiRNA plants. Branched trichomes (arrowheads) were visible on carpel valves of flowers in which *AG* function had been perturbed.

(C) Image of a flower from an ethanol-treated 35S$_{PRO}$:AlcR/AlcA$_{PRO}$:AG-amiRNA plant producing branched (arrowheads and inset) trichomes. A sepal was removed to aid visualization of the trichome phenotype.

(D) to **(G)** Scanning electron micrographs of the abaxial surfaces of carpel valves from wild-type (**[D]** and **[F]**) and ethanol-treated (**[E]** and **[G]**) 35S$_{PRO}$:AlcR/AlcA$_{PRO}$:AG-amiRNA plants.

(H) to **(J)** Scanning electron micrographs of the adaxial surface of a wild-type rosette leaf **(H)**, the abaxial surface of a wild-type sepal **(I)**, and the abaxial surface of a first-whorl organ of an *ap1-1* mutant flower **(J)**.

[See online article for color version of this figure.]

Notably, trichome formation on stamens and on carpels was never observed in the same flower (Figures 10C and 10D). While trichomes on stamens were found in flowers that were at an early stage of development when amiRNA expression was induced, flowers that showed trichomes on carpels had reached more intermediate stages. Thus, the competency of male and female reproductive organs for trichome initiation might be restricted to different stages of flower development.

In the experiments outlined above, we never observed the formation of trichomes on petals in response to B function perturbation despite the fact that *AP3/PI* are expressed in this organ type (Jack et al., 1992; Goto and Meyerowitz, 1994). Therefore, another pathway may exist in petals to suppress trichome initiation in the absence of B function activity.

TRY Suppresses Trichome Initiation in Parallel with *AG*

As described above, a specific knockdown of *AG* activity during intermediate stages of flower development led to the formation of several trichomes per gynoecium. This effect was relatively weak when compared, for example, to the aforementioned 35S$_{PRO}$:GL1 *try* plants, which are characterized by the formation of large numbers of trichomes on carpel valves (Schnittger et al., 1998). We therefore asked whether another pathway is involved in the suppression of trichome initiation on reproductive floral organs. Because it has been shown that the expression of *AP1* expands from whorls 1 and 2 into the center of the flower when *AG* function is disrupted (Gustafson-Brown et al., 1994), we tested whether AP1 could possibly suppress trichome initiation in the absence of C function. To this end, we activated *AG*-amiRNA expression in inflorescences of *ap1-1* null mutant plants. In this experiment, no

increase in trichome numbers on carpels was observed when compared with a perturbation of *AG* in wild-type inflorescences (see Supplemental Figure 5 online), suggesting that *AP1* is not involved in the suppression of trichome formation upon a loss of C function.

As mentioned above, *TRY* has been shown to play a role in controlling trichome initiation in flowers (Schnittger et al., 1998). We therefore analyzed the possible interplay between this repressor of trichome formation and *AG*. Because it had been reported previously (Wellmer et al., 2006) that *TRY* is upregulated at stages of early flower development during which the expression of *AG* commences (see Supplemental Figure 5 online), we first tested whether AG is involved in the control of *TRY* expression. An amiRNA-mediated knockdown of *AG* activity during early flower development showed that *TRY* expression is largely independent of *AG* (Figure 7B), suggesting that other factors promote its transcription. We next tested the effect of an amiRNA-mediated perturbation of *AG* activity in *try* mutant flowers, whose reproductive organs are typically trichomeless (Figure 10E). We found that, compared with wild-type flowers, the knockdown of *AG* activity in *try* mutants led to a strong increase in the number of trichomes formed on carpel valves (Figure 10F). These results together suggest that *TRY* suppresses trichome formation in parallel with *AG*.

DISCUSSION

In this study, we analyzed the mechanisms underlying the specification of reproductive floral organs by AG. We found that AG regulates the expression of a large number of genes, which
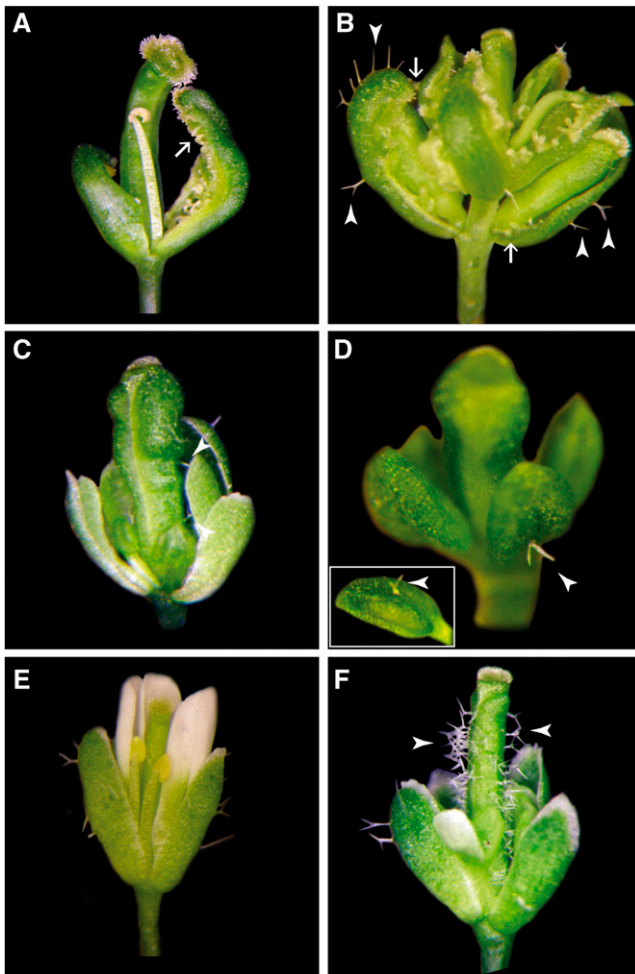
Figure 10. Trichome Initiation in Floral Reproductive Organs Is Suppressed by Redundant Pathways.

(A) and **(B)** $35S_{PRO}$:AlcR/AlcA$_{PRO}$:AG-amiRNA *ap2-2* flowers from untreated **(A)** and ethanol-treated **(B)** plants. Branched trichomes (arrowheads) were produced on the carpelloid first-whorl organs of treated plants, but not the first-whorl organs of untreated flowers. Arrows indicate the presence of stigmatic tissue and ectopic ovules on first-whorl organs.

(C) and **(D)** Effects of a simultaneous knockdown of B and C function activities. $35S_{PRO}$:GR-LhG4/6xOp$_{PRO}$:AG-amiRNA $35S_{PRO}$:AlcR/AlcA$_{PRO}$:PI-amiRNA plants were simultaneously treated with ethanol and dexamethasone to induce amiRNA expression.

(C) Flower, in which *PI* and *AG* were perturbed at approximately stages 7 to 9, with greenish petals and branched trichomes (arrowheads) on carpels.

(D) In flowers in which *PI* and *AG* function was perturbed at approximately stages 6 and 7, one or two branched trichomes (arrowheads) appeared intermittently on the abaxial surface of anthers. Inset in **(D)** shows the same trichome-bearing anther from the main panel from a different angle. In **(C)**, two sepals were removed, and in **(D)**, all sepals and petals were removed for visualization.

(E) and **(F)** $35S_{PRO}$:AlcR/AlcA$_{PRO}$:AG-amiRNA *try-29760* flowers from untreated **(E)** and ethanol-treated **(F)** plants.

(E) In untreated flowers, trichomes were present on sepals but not on any of the other floral organs.

are involved in a multitude of different developmental processes. Through the comparison of the ChIP-Seq results for AG with microarray data sets from *AG* perturbation experiments, we were able to identify high-confidence target genes and to distinguish between processes that are predominantly under direct or indirect control by AG. Among the direct targets, we found several known floral regulators that had not been previously associated with a direct regulation by AG, as well as many other genes with predicted regulatory functions. Thus, similar to what has been proposed for AP1 during floral initiation (Kaufmann et al., 2010), AG appears to serve as a hub in the flowering gene network that orchestrates reproductive floral organ specification to a large extent by controlling the expression of other regulatory genes.

The ChIP-Seq data for AG revealed that the transcription factor binds to the putative regulatory regions of almost 2000 genes during early flower development. At the same time, the results of the transcriptomics experiments we analyzed suggest that most (~88%) of these genes do not respond transcriptionally when the activity of AG is altered. Although similar observations have been made for other floral organ identity factors, the percentage of unresponsive genes is in the case of AG considerably larger than what has been reported for AP3/PI and AP1 (Kaufmann et al., 2010; Wuest et al., 2012). Through *AG* perturbation experiments in whole inflorescences we were able to show that some of these genes may be under the control of AG at more advanced floral stages. However, the number of these putative late targets is small and they cannot account for the hundreds of genes bound by AG that did not respond to an alteration of its activity during early flower development. While differences in the experimental and technical setups used for the different assays we considered for our analysis, as well as limitations in the detection of binding sites and of rare transcripts may be, at least in part, responsible for the limited overlap between the transcriptomics and ChIP-Seq data sets, it may also be indicative of complex responses of the flowering gene network to a perturbation of C function. For example, the apparent unresponsiveness of genes bound by AG in the *ag-1* loss-of-function experiments could be explained by the fact that many of them are also bound by AP1, as indicated by the considerable overlap of the ChIP-Seq data sets for these two MADS domain transcription factors (Figure 2). Thus, it appears possible that AP1 can interfere with the expression of AG target genes when it is present in the center of the flower and, in some cases, perhaps functionally replace AG, resulting in the absence of transcriptional differences when wild-type and *ag* mutant flowers are compared. However, in the previously published AG-GR gain-of-function experiments, which we also considered for our analysis and whose results again showed a limited overlap with those of the ChIP-Seq assays for AG, *AP1* was either mutated (Gómez-Mena et al., 2005) or repressed (Ito et al., 2004), suggesting that any effects of AP1 on AG target genes are not widespread.

(F) In ethanol-treated flowers, carpel valves were covered in stellate (three-branched) and double-branched trichomes (arrowheads).

[See online article for color version of this figure.]

When we compared the ChIP-Seq data for different MADS domain proteins involved in floral organ identity specification (Figure 2), we found that their binding patterns largely overlap. Therefore, it appears that these transcription factors can bind to many of the same sites in the *Arabidopsis* genome, in agreement with the idea that they have similar DNA binding specificities. Together with the observation that different floral organ identity factors have distinct sets of target genes (Kaufmann et al., 2009, 2010; Wuest et al., 2012), this finding suggests that sequence-specific DNA binding is only one input required for their functionality. In agreement with this idea are the results of a previous report, which showed that the expression of chimeric transcription factors, composed of the N-terminal DNA binding domains of heterologous MADS domain proteins and the C-terminal domains of floral organ identity factors, can rescue the corresponding floral homeotic mutants (Riechmann et al., 1996b). Because the C-terminal domains of MADS domain proteins are thought to be involved in mediating the formation of higher-order protein complexes (Riechmann et al., 1996a; Immink et al., 2010), this result suggests that another important input for floral organ identity factor function results from their interactions with as yet unidentified cofactors (Dornelas et al., 2011). In support of this conjecture, it has been reported that genomic regions bound by MADS domain proteins are not only enriched for CArG-boxes but also for several additional sequence motifs, of which some constitute known transcription factor binding sites (Kaufmann et al., 2009; Wuest et al., 2012). A recent proteomic analysis of floral MADS domain protein-containing complexes has identified several transcription factors of different families (Smaczniak et al., 2012), providing excellent cofactor candidates.

Through computational analysis, we detected a widespread derepression of genes that are most strongly expressed in leaf tissue in early-stage *ag* and *pi* mutant flowers (Figure 6). Furthermore, we found several known regulators of leaf development among genes controlled by AG. We therefore investigated whether the floral organ identity factors might suppress the leaf development program in floral primordia through the direct control of these regulatory genes. To this end, we focused on a group of activators and repressors of trichome initiation. We found that the observed changes in the expression of these genes after a perturbation of *AG* activity was consistent with a role of AG in the suppression of trichome formation. In agreement with this idea, a specific knockdown of *AG* activity in developing flowers led to the formation of branched trichomes on gynoecia and to the appearance of other leaf-like features on carpel valves (Figure 9). The former effect was considerably enhanced when the repressor of trichome initiation *TRY* was mutated, implying that at least two pathways are involved in the suppression of trichomes on reproductive floral organs. That a formation of trichomes was not observed on stamens after a perturbation of either C or B function despite the fact that both AP3/PI and AG can bind to the same set of regulators of trichome initiation (Figure 7A) suggested that these floral organ identity factors might act in a redundant manner in the suppression of trichome formation. In agreement with this idea, we found that a simultaneous knockdown of B and C function activities led to the formation of trichomes on anthers (Figure 10). Taken together, our data demonstrate that

AG and AP3/PI suppress the appearance of one characteristic leaf feature through the direct control of key regulatory genes. It remains to be elucidated whether the floral organ identity factors control other aspects of leaf development through similar mechanisms.

Our comparative analysis of the gene expression programs controlled by B and C function regulators showed that they control many processes in conjunction and often synergistically. However, we also found examples for antagonistic activities, most notably the direct control of many key regulators of carpel development, but also the differential regulation of individual genes involved in different developmental pathways. AG also appears to regulate distinct processes independently of B function. Examples are genes with known or suspected roles in DNA methylation, which are thought to act mainly in the silencing of transposons (Zheng et al., 2007; Feng et al., 2010; Borges et al., 2011; Stroud et al., 2013) and in DNA repair. While the exact function of these genes in the context of flower development is unknown, the fact that AG promotes their expression suggests that they may aid in the maintenance of genome integrity, which would be of particular importance during reproduction. Further experiments are currently in progress to understand the molecular mechanisms underlying the complex interactions we uncovered for the B and C function regulators and to understand their different modes of action.

METHODS

Plant Growth and Strains Used

Plants were grown on a soil:vermiculite:perlite (3:1:1) mixture at 20°C under constant illumination with cool white fluorescent light. Previously published *Arabidopsis thaliana* strains used in this study included the following: *ag-1* (Meyerowitz et al., 1989), *ap2-2* (Bowman et al., 1989), *ap1-1* (Irish and Sussex, 1990), $35S_{PRO}$:AP1-GR *ap1-1 cal-1* (Wellmer et al., 2006), $35S_{PRO}$:AlcR/AlcA$_{PRO}$:AP3-amiRNA $35S_{PRO}$:AP1-GR *ap1-1 cal-1*, $35S_{PRO}$:AlcR/AlcA$_{PRO}$:PI-amiRNA (Wuest et al., 2012), $35S_{PRO}$:AG-GR (Ito et al., 2004), and *try-29760* (Esch et al., 2003). $35S_{PRO}$:AP1-GR *ap1-1 cal-1 ag-1*, AG$_{PRO}$:AG-GFP AP1$_{PRO}$:AP1-GR *ap1-1 cal-1*, $35S_{PRO}$:AlcR/AlcA$_{PRO}$:AG-amiRNA, $35S_{PRO}$:AlcR/AlcA$_{PRO}$:AG-amiRNA AP1$_{PRO}$:AP1-GR *ap1-1 cal-1*, $35S_{PRO}$:GR-LhG4/6xOp$_{PRO}$:AG-amiRNA, $35S_{PRO}$:AlcR/AlcA$_{PRO}$:AG-amiRNA *try-29760*; $35S_{PRO}$:AlcR/AlcA$_{PRO}$:AG-amiRNA *ap2-2*, $35S_{PRO}$:AlcR/AlcA$_{PRO}$:AG-amiRNA *ap1-1*, and $35S_{PRO}$:GR-LhG4/6xOp$_{PRO}$:AG-amiRNA $35S_{PRO}$:AlcR/AlcA$_{PRO}$:PI-amiRNA plants were generated as described below.

Construction of AP1$_{PRO}$:AP1-GR Floral Induction System

To generate the AP1$_{PRO}$:AP1-GR construct, a genomic fragment containing the *AP1* locus was PCR amplified from Columbia-0 genomic DNA using primers DM-177/DM-180 (see Supplemental Table 2 online) and digested using *XhoI-XbaI*. The digested PCR fragment was then subcloned into pBJ36-GR treated with the same restriction enzymes. The AP1$_{PRO}$:AP1-GR translational fusion was then inserted into the plant transformation vector pML-BART (Eshed et al., 2001) using *NotI* restriction sites. Plant populations doubly homozygous for the *ap1-1* and *cal-1* mutant alleles were transformed using this pML-BART derivative. A transgenic line that responded to dexamethasone treatment by producing synchronous flower buds, sepals, and petals in the *ap1-1 cal-1* background was chosen for further experimentation. Plants homozygous for the AP1$_{PRO}$:AP1-GR transgene were subsequently identified.

Introduction of Inducible AG-amiRNA Transgenes into Mutant and Transgenic Backgrounds

$35S_{PRO}$:AlcR/AlcA$_{PRO}$:AG-amiRNA *try-29760*, $35S_{PRO}$:AlcR/AlcA$_{PRO}$:AG-amiRNA *ap2-2*, $35S_{PRO}$:AlcR/AlcA$_{PRO}$:AG-amiRNA $35S_{PRO}$:AlcR/AlcA$_{PRO}$:PI-amiRNA, and $35S_{PRO}$:AlcR/AlcA$_{PRO}$:AG-amiRNA *ap1-1* were generated by cross-pollination using parent strains that were homozygous for individual transgenes or mutations. The resulting F1 plants were allowed to self-pollinate, and the appropriate mutation/transgene combinations were isolated from the F2 populations through a combination of phenotyping, genotyping, and herbicide selection. Homozygous lines were identified through a combination of phenotyping, genotyping, and herbicide resistance. Primers used for genotyping are listed in Supplemental Table 2 online.

Plant Transformation

Agrobacterium tumefaciens–mediated plant transformation (using strain C58 pGV2260; McBride and Summerfelt, 1990) was performed using the floral dip method (Clough and Bent, 1998). Seedlings carrying pML-BART vector derivatives were identified by spraying with 200 µg/mL ammonium-glufosinate. For plants of accession Landsberg *erecta*, transformation was performed by applying a vacuum of 500 mbar for 5 min while inflorescences were submerged in the transformation solution.

Induction of Flower Development

For all experiments with the floral induction system, we used ~4-week-old AP1-GR *ap1-1 cal-1* plants. Flower development was induced as described (Wellmer et al., 2006) using a solution containing 10 µM dexamethasone (Sigma-Aldrich), 0.01% (v/v) ethanol, and 0.015% (v/v) Silwet L-77 (De Sangosse).

Induction of amiRNA Expression Using Ethanol Vapor

$35S_{PRO}$:AlcR/AlcA$_{PRO}$:amiRNA plants were transferred into trays that can be covered by plastic lids (18 cm × 32 cm × 50 cm). Two 50-mL tubes containing 10 mL of 100% ethanol each were placed near the plants before the lid was closed. For the mock treatments, ethanol was replaced with water.

Induction of amiRNA Expression Using Dexamethasone

The inflorescences of $35S_{PRO}$:GR-LhG4/6xOp$_{PRO}$:AG-amiRNA plants were treated with a solution containing 10 µM dexamethasone (Sigma-Aldrich), 0.01% (v/v) ethanol, and 0.015% (v/v) Silwet L-77 (De Sangosse). For mock treatments, dexamethasone was omitted.

Phenotypic Series of *AG* Perturbation

$35S_{PRO}$:AlcR/AlcA$_{PRO}$:AG-amiRNA plants were treated with five 3-h pulses of ethanol vapor; subsequently, flowers were observed every day and photographed at time of anthesis. Floral phenotypes were assessed with an Olympus SZX7 zoom stereomicroscope.

PCR Genotyping of the *ag-1* Allele

Genomic DNA was extracted from selected plants as described (Edwards et al., 1991) and used for PCR genotyping. Genotyping of *ag-1* in the absence of the AG$_{PRO}$:AG-GFP transgene was performed as described (Neff et al., 1998) with primers DM-178b and DM-179 (see Supplemental Table 2 online). Genotyping of *ag-1* in the presence of the AG$_{PRO}$:AG-GFP transgene was performed with primers DM-178b and DM-98 (see Supplemental Table 2 online). PCR products were digested with *Nla*III and *Afl*II. A band of ~500 bp was present in all digested samples, whereas

a band of ~220 bp indicated the presence of the *ag-1* mutation and a band of ~250 bp indicated the absence of the *ag-1* mutation.

RNA Preparation

Total RNA was isolated from tissue samples using the Plant Total RNA kit (Sigma-Aldrich). Quality of selected RNA samples was evaluated using a Bioanalyzer and a RNA Nano 6000 kit (Agilent).

Epidermal Surface Imaging

Epidermal surface imprints were generated as described (Horiguchi et al., 2006). Imaging was performed using an Olympus BX61 fluorescence microscope with differential interference contrast optics.

Epifluorescence Microscopy

GFP fluorescence was visualized with an Olympus BX61 fluorescence microscope with excitation wavelengths of 460/480 nm and emission wavelengths of 495 to 540 nm.

Confocal Imaging

Plants were grown on soil until bolting. The primary inflorescence was then removed and placed on growth medium, and all flowers older than stage 4-5 were dissected away from the meristem. Immediately prior to imaging, the specimen was stained with the vital dye FM4-64 (330 µg per mL) and imaged on a Zeiss LSM 510 confocal laser scanning microscope with a ×63 water immersion objective. Projections were generated with the Zeiss LSM browser software.

Scanning Electron Microscopy

Scanning electron micrographs were generated with the assistance of the Centre for Microscopy and Analysis (Trinity College Dublin, Ireland). Plant material was fixed for 2 h at room temperature with 3% glutaraldehyde (Sigma-Aldrich) in 0.05 M potassium phosphate buffer, pH 6.8. Samples were then washed six times with 0.05 M potassium phosphate buffer, pH 6.8, before being dehydrated gradually in an acetone series to 100% acetone at room temperature. Samples were then stored at 4°C in 100% acetone before being dried in liquid carbon dioxide at critical point. Samples were subsequently covered with 20 to 30 nm of gold using a sputter coater (Polaron SC500) and observed with a Tescan Mira XMU scanning electron microscope.

Detection of AG-GFP by Immunoblotting

Inflorescence tissue of AP1$_{PRO}$:AP1-GR AG$_{PRO}$:AG-GFP *ap1-1 cal-1* transgenic plants was collected 4 d after treatment with a dexamethasone-containing solution. Nuclear extracts from plants were prepared from this tissue as described previously (Kaufmann et al., 2010). Proteins were separated on a 10% SDS-PAGE gel, followed by transfer to a polyvinylidene difluoride membrane. The AG-GFP fusion protein was detected using a rabbit antibody (Ab290; Abcam) diluted 4000-fold in PBS-T (1 × PBS with 0.05% [v/v] Tween 20) supplemented with 5% (w/v) milk.

Quantitative RT-PCR Experiments

Total RNA extracts were treated with the DNA-free kit (Ambion) to remove genomic DNA contamination. cDNA synthesis was performed using these RNA preparations, oligo(dT) primers, and the RevertAid H Minus M-MuLV reverse transcriptase (Fermentas). Relative transcript abundance of selected genes (see Supplemental Table 3 online for a list of genes and the primers used) was determined using the Roche LightCycler 480 system

and the LC480 SYBR Green I Master kit (Roche Applied Sciences). Measurements were taken for three biologically independent sets of samples. In addition, all PCR reactions were performed twice for each cDNA (technical duplicates). LightCycler melting curves were obtained for the reactions, revealing single peak melting curves for all amplification products. The amplification data were analyzed using the second derivative maximum method, and resulting Cp values were converted into relative expression values using the comparative cycle threshold method (Livak and Schmittgen, 2001). Two reference genes (*REF1* and *REF3*; see Supplemental Table 3 online) (Czechowski et al., 2005) were used to normalize the data. Their Cp values were averaged for each sample.

Chromatin Immunoprecipitation and Next-Generation Sequencing

For the identification of AG binding sites, we collected inflorescence tissue from ~4-week-old AG$_{PRO}$:AG-GFP AP1$_{PRO}$:AP1-GR *ap1-1 cal-1 ag-1* plants, as well as from 35S$_{PRO}$:AP1-GR *ap1-1 cal-1* plants (as background control), 4 d after induction of flower development through treatment with a solution containing 10 μM dexamethasone (Sigma-Aldrich), 0.01% (v/v) ethanol, and 0.015% (v/v) Silwet L-77 (De Sangosse). ChIP experiments with GFP-specific antibodies (Ab290; Abcam) and next-generation sequencing of the precipitated genomic DNA were done as previously described (Wuest et al., 2012). For each of genotype used, two libraries were generated from independently obtained immunoprecipitated genomic DNA and sequenced. For the AG-GFP ChIP-Seq replicates, we calculated a Pearson correlation coefficient of mean signals in nonoverlapping 1-kb windows as previously described (Kaufmann et al., 2010) and obtained a value of 0.88, indicating high reproducibility of the binding data.

ChIP–Quantitative PCR Experiments

Tissue was collected from ~4-week-old AP1$_{PRO}$:AP1-GR AG$_{PRO}$:AG-GFP *ap1-1 cal-1 ag-1* and AP1$_{PRO}$:AP1-GR *ap1-1 cal-1* plants 4 d after dexamethasone treatment. ChIP was performed as described (Wuest et al., 2012), using 2 μL of a GFP antibody (A6455; Invitrogen) that was different from that used in the ChIP-Seq experiments. Relative DNA abundance of selected genomic regions (see Supplemental Table 4 online for a list of genes and the primers used) was then determined using the Roche LightCycler 480 system and the LC480 SYBR Green I Master kit (Roche Applied Sciences). Measurements were taken for four biologically independent sets of samples. LightCycler melting curves were obtained for the reactions, revealing single peak melting curves for all amplification products. The amplification data were analyzed using the second derivative maximum method, and resulting Cp values were converted into relative enrichment values using the comparative cycle threshold method where input DNA was used to normalize the data (Livak and Schmittgen, 2001). The input DNA was a sample of the chromatin available for precipitation that was extracted prior to the addition of antibody to account for differences in the solubility of different genomic regions, the shearing of DNA, and amplification. Four genomic reference regions (ACT7, REF1 [Kaufmann et al., 2010], Mu [Chae et al., 2008], and TUB3) were used to normalize the data. Their Cp values were averaged for each sample.

Publicly Available ChIP-Seq Data Sets

Short sequence read data sets from ChIP-Seq experiments for AP1 (Kaufmann et al., 2010), SEP3 (Kaufmann et al., 2009), and AP2 (Yant et al., 2010) were downloaded from the National Center for Biotechnology Information SRA database (www.ncbi.nlm.nih.gov/sra) and sequence information from the SRA files dumped into fastq files using the Sratoolkit software (version 2.0.1) as described in the manual at www.ncbi.nlm.nih. gov/books/NBK47540. In some cases, the read numbers or qualities of replicates in these reference data sets were found to vary slightly: From the SEP3 data set, only replicate 1 was used. Quality control of the

sequenced libraries was performed using the FastQC software (www. bioinformatics.bbsrc.ac.uk/projects/fastqc/).

Peak Calling and Publicly Available Binding Data

Peak calling for the ChIP-Seq experiments was performed using the CSAR package (Muiño et al., 2011), and enriched regions were identified at a false discovery rate (FDR) < 0.001 (with five rounds of permutations for each data set, resulting in >600,000 permutations). Default parameters were used. Only peak regions with stretches of >50 bp were retained.

Peaks were associated with genes using *CSAR* functionality, whereby a peak had to reside in a genomic region ranging from 3 kb upstream of a gene's transcriptional start position to 1 kb downstream of its transcriptional end position. Gene range definitions were downloaded from The Arabidopsis Information Resource (TAIR; file: TAIR10_GFF3_genes. gff). GO term enrichments were performed as described for the microarray analyses by using GO mappings provided in the org.At.tair.db data package (version 2.6.4) downloaded from the Bioconductor homepage. Visualization of genomic regions was performed using the Genome-Graphs package version 1.14.0 (Durinck et al., 2009).

SEP3 binding site definitions were kindly provided by Dr. Jose Muino via the Pri-Cat homepage (www.ab.wur.nl/pricat/). Hexagonal binning routines from the R package hexbin (version 1.26.0) were used in plots that show correlated binding around common target genes.

Merging Data from Biological ChIP-Seq Replicates

In order to merge biological replicates from the AG-GFP ChIP-Seq experiments, peak definitions determined for AG-GFP replicate 2 were retained only if they showed any overlap with the AG-GFP replicate 1. Because the AG-GFP replicate 1 showed lower enrichment values than AG-GFP replicate 2, the significantly enriched regions were extended by 25 bp in either direction before the overlaps with replicate 2 were determined.

Calculation of Relative Enrichment Scores of ChIP-Seq Data

Determination of per-base enrichment scores for the heat maps showing relative enrichment around AG and PI binding sites was performed using custom *R* scripts. For this, the per-base enrichment scores based on a Poisson distribution were calculated by the *CSAR* package. Subsequently, the enrichment score cutoff for peak detection, at a FDR of 0.001, was determined using five rounds of permutations. This score was used as a normalization factor, and per-base enrichment scores were divided by this normalization factor (so that a normalized enrichment score of 1 denotes the enrichment score at an FDR of 0.001 and a normalized score of 2 denotes twice this score, etc.). Normalized scores higher than 5 were truncated to the value of 5 for better visualization.

Detection of Motifs Present at Putative AG Binding Sites

For the detection of motifs at putative AG binding sites, 400-bp core sequences centered around peak locations were submitted to the browser-based MEME-ChIP analysis suite (http://meme.sdsc.edu/meme/) (Bailey et al., 2009). Position weight matrices from the MEME software output (Bailey and Elkan, 1994) were matched using the matchPWM function (as implemented in the Bioconductor package Biostrings) and a minimum score of 80%.

Microarray Experiments and Data Analysis

For the *ag-1* microarray experiments, we collected inflorescence-like meristems from 35S$_{PRO}$:AP1-GR *ap1-1 cal-1* plants segregating the *ag-1*

allele immediately before applying a dexamethasone-containing solution (as described above) to induce flower development, as well as 2.5 (equivalent to approximately stage 3-4) and 5 d (corresponding to approximately stage 6) after dexamethasone treatment. Tissue from ~80 plants per time point was collected into individual tubes and temporarily stored at −80°C. Subsequently, floral phenotypes of each plant used for the tissue collection were determined to infer the genotype. When the results of this approach were inconclusive, PCR-based genotyping of the *ag-1* allele was performed as described above. The tissue from ~20 individual plants identified as being homozygous for *ag-1* was pooled for each time point taken. In addition, tissue from plants that formed wild-type-like flowers was also combined, resulting in control samples. In total, four biologically independent sets of samples were generated for each time point. RNA was isolated from the *ag-1* mutant and from wild-type-like flowers as described above and was cohybridized to custom-designed microarrays (Agilent) as previously described (Kaufmann et al., 2010).

For the 35S$_{PRO}$:GR-LhG4/6xOp$_{PRO}$:AG-amRNA microarray experiments, we collected floral buds from stages 1 to 10 (approximately) from ~25 plants 24 h after treatment with a dexamethasone-containing or mock solution as described above. Four biological replicates were generated for each treatment. RNA was isolated from the dexamethasone-treated and mock-treated flowers as described above, and was cohybridized to custom-designed microarrays (Agilent) as previously described (Kaufmann et al., 2010).

Microarray Data Analysis and Probe Reannotation

Probes on the Agilent array (their design was based on the *Arabidopsis* genome release version 8) were reannotated to match version 10 as described previously (Wuest et al., 2012). Low-level data processing was performed using functionality provided by Limma version 2.14.0 (Silver et al., 2009). Agilent median signals and background were read into *R* and background correction was performed using the backgroundCorrect function (Ritchie et al., 2007) with maximum likelihood estimation of the background (Silver et al., 2009) and an offset of 50. Between-channel normalization was performed using loess normalization and between-array normalization using quantile normalization (Smyth and Speed, 2003). Signals of probes targeting transcripts from the same locus were averaged using the avereps function provided in the Limma package. Nonspecific filtering was performed using the Genefilter package version 1.36.0, based on a signal cutoff determined by the median signal from negative probe signals (i.e., probes that do not match genomic or transcript sequences according to the *Arabidopsis* TAIR10 genome release), so that only those probes with higher signals in at least three arrays were retained.

Base-level annotations were retrieved from the Bioconductor homepage (package Arabidopsis.db0 version 2.6.4) and an annotation package for the custom-made 44K Agilent array was generated using AnnotationDbi package (version 1.16.10). GO terms contained within the "biological process" class were used for further analyses, and terms with less than nine associated genes were removed. In order to reduce the number of statistical tests performed for GO analyses, redundancy between closely related terms was eliminated as follows: Parent terms were removed if they had more than 90% gene association overlaps with the combination of their daughter terms.

Pfam and Gene family information was retrieved from the TAIR homepage (files gene_families_sep_29_09_update.txt and TAIR10_all.domains). *Arabidopsis* gene identifiers for the gene family record of the "B3 transcription factor family" were missing and therefore manually updated according to the previously proposed naming scheme (Romanel et al., 2009). Only families with nine or more associated genes were included in the analysis. Redundancies among protein families were removed by searching for protein families that had more than 90% overlaps in gene associations with another family and removing the smaller family

from further analyses. The same procedure was used to remove redundant gene families.

Testing for differential gene expression was performed using linear models (Smyth, 2004) as described in the Limma user guide. Our data analysis mainly focused on functional groups of genes (e.g., GO terms, gene/protein families) overrepresented within lists of potentially misexpressed genes. Therefore, the multiple testing adjustments were performed at the level of enrichment tests rather than at the level of selection of differentially expressed genes. Our gene selection strategy was based on declaring a gene as differentially expressed at a P value < 0.01. GO term enrichment analyses and protein/gene family enrichment analyses were performed using a two-sided Fisher's exact test implemented in R. Adjustments for multiple testing were performed using the p.adjust function in R, using Benjamini and Hochberg adjustments (Benjamini and Hochberg, 1995).

To test for coordinated changes of gene expression within selected functional groups, gene set enrichment analysis was performed using the mroast function as implemented in the Limma package (Wu et al., 2010) with 10,000 rotations and "msq" summary set statistic that is sensitive to smaller proportions of differentially expressed genes within gene sets. Heat maps were generated using the gplots package version 2.10.1.

For the comparison of the *ag-1* microarray data with the domain-specific expression data from Jiao and Meyerowitz (2010), we first calculated, for each of the 1047 differentially expressed genes, the ratio between mean signal intensities in the *ag-1* and wild-type channels across all time points to identify genes that show a general trend toward up- or downregulation in response to *AG* perturbation. We then compared this gene list to a list of genes that are differentially expressed (defined by a P value <0.01 and a fold change >2) between the *AP1* expression domain and the *AG* expression domain at floral stage 4 or 6-7. For the up- and downregulated genes separately, we then calculated the mean of the log$_2$-transformed fold-change ratios (as provided in the Jiao and Meyerowitz [2010] data set). At floral stage 4, the mean log$_2$-transformed fold change ratio for the downregulated genes was −0.74 and 0.93 for the upregulated genes. At stage 6-7, the ratios were −0.41 and 1.24, respectively.

Calculation of Gene Expression Signals across an *Arabidopsis* Tissue Atlas

A set of selected microarray data sets from the analysis of gene expression in different *Arabidopsis* tissue and cell types was downloaded from public repositories (see Supplemental Data Set 4 online for details). This set contains data from a study of a variety of *Arabidopsis* tissues (Schmid et al., 2005), root cell types (Birnbaum et al., 2003; Brady et al., 2007), pollen of different developmental stages (Honys and Twell, 2004), as well as data from discrete seed compartments (as used in Le et al., 2010); ArrayExpress data set GSE12404, www.ebi.ac.uk/arrayexpress), cell types of the shoot apical meristem (Yadav et al., 2009), sperm cells (Borges et al., 2008), female gametophytic cell types (Wuest et al., 2010), and ovules (Yu et al., 2005). In total, the tissue atlas includes expression data for 65 tissue types of gametophytic, sporophytic, and embryonic origin. Gene expression signals were calculated using dChIP (version 2010) using invariant-set normalization and a PM-only model. Probe set definitions according to a newer *Arabidopsis* genome release (TAIR9) were used as described previously (Schmidt et al., 2011). Mean signals were calculated for biological replicates, and tissue/cell types were classified into tissue classes (e.g., root/leaf/gametophye, etc.; see Supplemental Data Set 4 online). We examined expression peaks across the tissue atlas and used these as a proxy for preferential expression in a tissue class. To compare observed with expected expression peak numbers, we likewise analyzed 100,000 equally sized gene sets randomly selected from the genes represented on the microarrays.

Accession Numbers

Sequence data from this article can be found in the GenBank/EMBL data libraries under accession numbers listed in Supplemental Table 5 online.

Supplemental Data

The following materials are available in the online version of this article.

Supplemental Figure 1. Generation and Characterization of AG-GFP Lines.

Supplemental Figure 2. Identification of AG Response Genes through Microarray Analysis.

Supplemental Figure 3. Processes Regulated by AG.

Supplemental Figure 4. Comparison of the Processes Controlled by the B and C Function Regulators.

Supplemental Figure 5. Control of Trichome Initiation by Redundant Pathways.

Supplemental Table 1. Artificial miRNAs Directed against *AG*.

Supplemental Table 2. Primers Used for PCR Genotyping and Generation of Constructs.

Supplemental Table 3. Primers Used for qRT-PCR Analysis.

Supplemental Table 4. Primers Used for ChIP-qPCR Analysis.

Supplemental Table 5. Genes Discussed in This Study.

Supplemental Data Set 1. Genomic Regions Identified as Enriched in the AG-GFP ChIP-Seq Experiments.

Supplemental Data Set 2. Genes Identified as Differentially Expressed in the Microarray Experiments.

Supplemental Data Set 3. GO Terms and Gene Families/Protein Motifs Identified as Significantly Enriched or Underrepresented among Differentially Expressed Genes.

Supplemental Data Set 4. Microarray Data Sets Used to Construct an *Arabidopsis* Expression Atlas.

AUTHOR CONTRIBUTIONS

S.E.W., D.S.O., E.G., and F.W. designed the research and wrote the article. All authors performed research. S.E.W., D.S.O., P.T.R., E.G., and F.W. analyzed data.

REFERENCES

Bailey, T.L., Boden, M., Buske, F.A., Frith, M., Grant, C.E., Clementi, L., Ren, J., Li, W.W., and Noble, W.S. (2009). MEME SUITE: Tools for motif discovery and searching. Nucleic Acids Res. **37** (Web Server issue)**:** W202–W208.

Bailey, T.L., and Elkan, C. (1994). Fitting a mixture model by expectation maximization to discover motifs in biopolymers. In Proceedings of the Second International Conference on Intelligent Systems for Molecular Biology, (Menlo Park, California: AAAI Press), pp. 28–36.

Benjamini, Y., and Hochberg, Y. (1995). Controlling the false discovery rate - A practical and powerful approach to multiple testing. J. R. Stat. Soc. B **57:** 289–300.

Birnbaum, K., Shasha, D.E., Wang, J.Y., Jung, J.W., Lambert, G.M., Galbraith, D.W., and Benfey, P.N. (2003). A gene expression map of the *Arabidopsis* root. Science **302:** 1956–1960.

Borges, F., Gomes, G., Gardner, R., Moreno, N., McCormick, S., Feijó, J.A., and Becker, J.D. (2008). Comparative transcriptomics of *Arabidopsis* sperm cells. Plant Physiol. **148:** 1168–1181.

Borges, F., Pereira, P.A., Slotkin, R.K., Martienssen, R.A., and Becker, J.D. (2011). MicroRNA activity in the *Arabidopsis* male germline. J. Exp. Bot. **62:** 1611–1620.

Bowman, J.L., Smyth, D.R., and Meyerowitz, E.M. (1989). Genes directing flower development in *Arabidopsis*. Plant Cell **1:** 37–52.

Bowman, J.L., Smyth, D.R., and Meyerowitz, E.M. (1991). Genetic interactions among floral homeotic genes of *Arabidopsis*. Development **112:** 1–20.

Brady, S.M., Orlando, D.A., Lee, J.Y., Wang, J.Y., Koch, J., Dinneny, J.R., Mace, D., Ohler, U., and Benfey, P.N. (2007). A high-resolution root spatiotemporal map reveals dominant expression patterns. Science **318:** 801–806.

Breuil-Broyer, S., Morel, P., de Almeida-Engler, J., Coustham, V., Negrutiu, I., and Trehin, C. (2004). High-resolution boundary analysis during *Arabidopsis thaliana* flower development. Plant J. **38:** 182–192.

Chae, E., Tan, Q.K., Hill, T.A., and Irish, V.F. (2008). An *Arabidopsis* F-box protein acts as a transcriptional co-factor to regulate floral development. Development **135:** 1235–1245.

Clough, S.J., and Bent, A.F. (1998). Floral dip: A simplified method for Agrobacterium-mediated transformation of *Arabidopsis thaliana*. Plant J. **16:** 735–743.

Coen, E.S., and Meyerowitz, E.M. (1991). The war of the whorls: Genetic interactions controlling flower development. Nature **353:** 31–37.

Czechowski, T., Stitt, M., Altmann, T., Udvardi, M.K., and Scheible, W.R. (2005). Genome-wide identification and testing of superior reference genes for transcript normalization in *Arabidopsis*. Plant Physiol. **139:** 5–17.

Deveaux, Y., Peaucelle, A., Roberts, G.R., Coen, E., Simon, R., Mizukami, Y., Traas, J., Murray, J.A.H., Doonan, J.H., and Laufs, P. (2003). The ethanol switch: A tool for tissue-specific gene induction during plant development. Plant J. **36:** 918–930.

Ditta, G., Pinyopich, A., Robles, P., Pelaz, S., and Yanofsky, M.F. (2004). The SEP4 gene of *Arabidopsis thaliana* functions in floral organ and meristem identity. Curr. Biol. **14:** 1935–1940.

Dornelas, M.C., Patreze, C.M., Angenent, G.C., and Immink, R.G. (2011). MADS: The missing link between identity and growth? Trends Plant Sci. **16:** 89–97.

Drews, G.N., Bowman, J.L., and Meyerowitz, E.M. (1991). Negative regulation of the *Arabidopsis* homeotic gene AGAMOUS by the APETALA2 product. Cell **65:** 991–1002.

Durinck, S., Bullard, J., Spellman, P.T., and Dudoit, S. (2009). GenomeGraphs: Integrated genomic data visualization with R. BMC Bioinformatics **10:** 2.

Edwards, K., Johnstone, C., and Thompson, C. (1991). A simple and rapid method for the preparation of plant genomic DNA for PCR analysis. Nucleic Acids Res. **19:** 1349.

Esch, J.J., Chen, M., Sanders, M., Hillestad, M., Ndkium, S., Idelkope, B., Neizer, J., and Marks, M.D. (2003). A contradictory

GLABRA3 allele helps define gene interactions controlling trichome development in *Arabidopsis*. Development **130:** 5885–5894.

Eshed, Y., Baum, S.F., Perea, J.V., and Bowman, J.L. (2001). Establishment of polarity in lateral organs of plants. Curr. Biol. **11:** 1251–1260.

Feng, S., Jacobsen, S.E., and Reik, W. (2010). Epigenetic reprogramming in plant and animal development. Science **330:** 622–627.

Gan, Y., Liu, C., Yu, H., and Broun, P. (2007). Integration of cytokinin and gibberellin signalling by *Arabidopsis* transcription factors GIS, ZFP8 and GIS2 in the regulation of epidermal cell fate. Development **134:** 2073–2081.

Gómez-Mena, C., de Folter, S., Costa, M.M., Angenent, G.C., and Sablowski, R. (2005). Transcriptional program controlled by the floral homeotic gene AGAMOUS during early organogenesis. Development **132:** 429–438.

Goto, K., and Meyerowitz, E.M. (1994). Function and regulation of the *Arabidopsis* floral homeotic gene PISTILLATA. Genes Dev. **8:** 1548–1560.

Gremski, K., Ditta, G., and Yanofsky, M.F. (2007). The HECATE genes regulate female reproductive tract development in *Arabidopsis thaliana*. Development **134:** 3593–3601.

Gustafson-Brown, C., Savidge, B., and Yanofsky, M.F. (1994). Regulation of the *Arabidopsis* floral homeotic gene APETALA1. Cell **76:** 131–143.

Honma, T., and Goto, K. (2001). Complexes of MADS-box proteins are sufficient to convert leaves into floral organs. Nature **409:** 525–529.

Honys, D., and Twell, D. (2004). Transcriptome analysis of haploid male gametophyte development in *Arabidopsis*. Genome Biol. **5:** R85.

Horiguchi, G., Fujikura, U., Ferjani, A., Ishikawa, N., and Tsukaya, H. (2006). Large-scale histological analysis of leaf mutants using two simple leaf observation methods: Identification of novel genetic pathways governing the size and shape of leaves. Plant J. **48:** 638–644.

Hueber, S.D., and Lohmann, I. (2008). Shaping segments: Hox gene function in the genomic age. Bioessays **30:** 965–979.

Immink, R.G., Kaufmann, K., and Angenent, G.C. (2010). The 'ABC' of MADS domain protein behaviour and interactions. Semin. Cell Dev. Biol. **21:** 87–93.

Irish, V.F., and Sussex, I.M. (1990). Function of the apetala-1 gene during *Arabidopsis* floral development. Plant Cell **2:** 741–753.

Ito, T., Ng, K.H., Lim, T.S., Yu, H., and Meyerowitz, E.M. (2007). The homeotic protein AGAMOUS controls late stamen development by regulating a jasmonate biosynthetic gene in *Arabidopsis*. Plant Cell **19:** 3516–3529.

Ito, T., Wellmer, F., Yu, H., Das, P., Ito, N., Alves-Ferreira, M., Riechmann, J.L., and Meyerowitz, E.M. (2004). The homeotic protein AGAMOUS controls microsporogenesis by regulation of SPOROCYTELESS. Nature **430:** 356–360.

Jack, T., Brockman, L.L., and Meyerowitz, E.M. (1992). The homeotic gene APETALA3 of *Arabidopsis thaliana* encodes a MADS box and is expressed in petals and stamens. Cell **68:** 683–697.

Jiao, Y., and Meyerowitz, E.M. (2010). Cell-type specific analysis of translating RNAs in developing flowers reveals new levels of control. Mol. Syst. Biol. **6:** 419.

Jofuku, K.D., den Boer, B.G., Van Montagu, M., and Okamuro, J.K. (1994). Control of *Arabidopsis* flower and seed development by the homeotic gene APETALA2. Plant Cell **6:** 1211–1225.

Kaufmann, K., Muiño, J.M., Jauregui, R., Airoldi, C.A., Smaczniak, C., Krajewski, P., and Angenent, G.C. (2009). Target genes of the MADS transcription factor SEPALLATA3: Integration of developmental and hormonal pathways in the *Arabidopsis* flower. PLoS Biol. **7:** e1000090.

Kaufmann, K., Wellmer, F., Muiño, J.M., Ferrier, T., Wuest, S.E., Kumar, V., Serrano-Mislata, A., Madueño, F., Krajewski, P., Meyerowitz, E.M., Angenent, G.C., and Riechmann, J.L. (2010). Orchestration of floral initiation by APETALA1. Science **328:** 85–89.

Krizek, B.A., Lewis, M.W., and Fletcher, J.C. (2006). RABBIT EARS is a second-whorl repressor of AGAMOUS that maintains spatial boundaries in *Arabidopsis* flowers. Plant J. **45:** 369–383.

Larkin, J.C., Oppenheimer, D.G., Lloyd, A.M., Paparozzi, E.T., and Marks, M.D. (1994). Roles of the GLABROUS1 and TRANSPARENT TESTA GLABRA genes in *Arabidopsis* trichome development. Plant Cell **6:** 1065–1076.

Law, J.A., and Jacobsen, S.E. (2010). Establishing, maintaining and modifying DNA methylation patterns in plants and animals. Nat. Rev. Genet. **11:** 204–220.

Le, B.H., et al. (2010). Global analysis of gene activity during *Arabidopsis* seed development and identification of seed-specific transcription factors. Proc. Natl. Acad. Sci. USA **107:** 8063–8070.

Liljegren, S.J., Ditta, G.S., Eshed, Y., Savidge, B., Bowman, J.L., and Yanofsky, M.F. (2000). SHATTERPROOF MADS-box genes control seed dispersal in *Arabidopsis*. Nature **404:** 766–770.

Liu, X., Kim, Y.J., Müller, R., Yumul, R.E., Liu, C., Pan, Y., Cao, X., Goodrich, J., and Chen, X. (2011). AGAMOUS terminates floral stem cell maintenance in *Arabidopsis* by directly repressing WUSCHEL through recruitment of Polycomb Group proteins. Plant Cell **23:** 3654–3670.

Livak, K.J., and Schmittgen, T.D. (2001). Analysis of relative gene expression data using real-time quantitative PCR and the 2(-Delta Delta C(T)) method. Methods **25:** 402–408.

Mandel, M.A., Gustafson-Brown, C., Savidge, B., and Yanofsky, M.F. (1992). Molecular characterization of the *Arabidopsis* floral homeotic gene APETALA1. Nature **360:** 273–277.

Matias-Hernandez, L., Battaglia, R., Galbiati, F., Rubes, M., Eichenberger, C., Grossniklaus, U., Kater, M.M., and Colombo, L. (2010). VERDANDI is a direct target of the MADS domain ovule identity complex and affects embryo sac differentiation in *Arabidopsis*. Plant Cell **22:** 1702–1715.

McBride, K.E., and Summerfelt, K.R. (1990). Improved binary vectors for Agrobacterium-mediated plant transformation. Plant Mol. Biol. **14:** 269–276.

Meyerowitz, E.M., Smyth, D.R., and Bowman, J.L. (1989). Abnormal flowers and pattern formation in floral development. Development **106:** 209–217.

Muiño, J.M., Kaufmann, K., van Ham, R.C., Angenent, G.C., and Krajewski, P. (2011). ChIP-seq Analysis in R (CSAR): An R package for the statistical detection of protein-bound genomic regions. Plant Methods **7:** 11.

Neff, M.M., Neff, J.D., Chory, J., and Pepper, A.E. (1998). dCAPS, a simple technique for the genetic analysis of single nucleotide polymorphisms: Experimental applications in *Arabidopsis thaliana* genetics. Plant J. **14:** 387–392.

Pelaz, S., Tapia-López, R., Alvarez-Buylla, E.R., and Yanofsky, M.F. (2001). Conversion of leaves into petals in *Arabidopsis*. Curr. Biol. **11:** 182–184.

Riechmann, J.L., Krizek, B.A., and Meyerowitz, E.M. (1996a). Dimerization specificity of *Arabidopsis* MADS domain homeotic proteins APETALA1, APETALA3, PISTILLATA, and AGAMOUS. Proc. Natl. Acad. Sci. USA **93:** 4793–4798.

Riechmann, J.L., Wang, M., and Meyerowitz, E.M. (1996b). DNA-binding properties of *Arabidopsis* MADS domain homeotic proteins APETALA1, APETALA3, PISTILLATA and AGAMOUS. Nucleic Acids Res. **24:** 3134–3141.

Ritchie, M.E., Silver, J., Oshlack, A., Holmes, M., Diyagama, D., Holloway, A., and Smyth, G.K. (2007). A comparison of background correction methods for two-colour microarrays. Bioinformatics **23:** 2700–2707.

Romanel, E.A., Schrago, C.G., Couñago, R.M., Russo, C.A., and Alves-Ferreira, M. (2009). Evolution of the B3 DNA binding superfamily: new insights into REM family gene diversification. PLoS ONE **4:** e5791.

Roslan, H.A., Salter, M.G., Wood, C.D., White, M.R., Croft, K.P., Robson, F., Coupland, G., Doonan, J., Laufs, P., Tomsett, A.B., and Caddick, M.X. (2001). Characterization of the ethanol-inducible alc gene-expression system in *Arabidopsis thaliana*. Plant J. **28:** 225–235.

Sablowski, R. (2010). Genes and functions controlled by floral organ identity genes. Semin. Cell Dev. Biol. **21:** 94–99.

Sakai, H., Krizek, B.A., Jacobsen, S.E., and Meyerowitz, E.M. (2000). Regulation of SUP expression identifies multiple regulators involved in *Arabidopsis* floral meristem development. Plant Cell **12:** 1607–1618.

Savidge, B., Rounsley, S.D., and Yanofsky, M.F. (1995). Temporal relationship between the transcription of two *Arabidopsis* MADS box genes and the floral organ identity genes. Plant Cell **7:** 721–733.

Schellmann, S., Schnittger, A., Kirik, V., Wada, T., Okada, K., Beermann, A., Thumfahrt, J., Jürgens, G., and Hülskamp, M. (2002). TRIPTYCHON and CAPRICE mediate lateral inhibition during trichome and root hair patterning in *Arabidopsis*. EMBO J. **21:** 5036–5046.

Schmid, M., Davison, T.S., Henz, S.R., Pape, U.J., Demar, M., Vingron, M., Schölkopf, B., Weigel, D., and Lohmann, J.U. (2005). A gene expression map of *Arabidopsis thaliana* development. Nat. Genet. **37:** 501–506.

Schmidt, A., Wuest, S.E., Vijverberg, K., Baroux, C., Kleen, D., and Grossniklaus, U. (2011). Transcriptome analysis of the *Arabidopsis* megaspore mother cell uncovers the importance of RNA helicases for plant germline development. PLoS Biol. **9:** e1001155.

Schnittger, A., Jürgens, G., and Hülskamp, M. (1998). Tissue layer and organ specificity of trichome formation are regulated by GLABRA1 and TRIPTYCHON in *Arabidopsis*. Development **125:** 2283–2289.

Schwab, R., Ossowski, S., Riester, M., Warthmann, N., and Weigel, D. (2006). Highly specific gene silencing by artificial microRNAs in *Arabidopsis*. Plant Cell **18:** 1121–1133.

Silver, J.D., Ritchie, M.E., and Smyth, G.K. (2009). Microarray background correction: Maximum likelihood estimation for the normal-exponential convolution. Biostatistics **10:** 352–363.

Smaczniak, C., et al. (2012). Characterization of MADS-domain transcription factor complexes in *Arabidopsis* flower development. Proc. Natl. Acad. Sci. USA **109:** 1560–1565.

Smyth, D.R., Bowman, J.L., and Meyerowitz, E.M. (1990). Early flower development in *Arabidopsis*. Plant Cell **2:** 755–767.

Smyth, G.K. (2004). Linear models and empirical Bayes methods for assessing differential expression in microarray experiments. Stat. Appl. Genet. Mol. Biol. **3:** Article3.

Smyth, G.K., and Speed, T. (2003). Normalization of cDNA microarray data. Methods **31:** 265–273.

Steiner, E., Efroni, I., Gopalraj, M., Saathoff, K., Tseng, T.S., Kieffer, M., Eshed, Y., Olszewski, N., and Weiss, D. (2012). The *Arabidopsis* O-linked N-acetylglucosamine transferase SPINDLY interacts with class I TCPs to facilitate cytokinin responses in leaves and flowers. Plant Cell **24:** 96–108.

Stroud, H., Greenberg, M.V., Feng, S., Bernatavichute, Y.V., and Jacobsen, S.E. (2013). Comprehensive analysis of silencing mutants reveals complex regulation of the *Arabidopsis* methylome. Cell **152:** 352–364.

Sun, B., Xu, Y., Ng, K.H., and Ito, T. (2009). A timing mechanism for stem cell maintenance and differentiation in the *Arabidopsis* floral meristem. Genes Dev. **23:** 1791–1804.

Sundström, J.F., Nakayama, N., Glimelius, K., and Irish, V.F. (2006). Direct regulation of the floral homeotic APETALA1 gene by APETALA3 and PISTILLATA in *Arabidopsis*. Plant J. **46:** 593–600.

Theissen, G., Becker, A., Winter, K.U., Muenster, T., Kirchner, C., and Saedler, H. (2002). How the Land Plants Learned Their Floral ABCs: The role of MADS Box Genes in the Evolutionary Origin of Flowers. (London: Taylor & Francis).

von Goethe, J.W. (1790) Versuch die Metamorphose der Pflanzen zu erklären. (Gotha, Germany: Ettinger).

Wang, S., Kwak, S.H., Zeng, Q., Ellis, B.E., Chen, X.Y., Schiefelbein, J., and Chen, J.G. (2007). TRICHOMELESS1 regulates trichome patterning by suppressing GLABRA1 in *Arabidopsis*. Development **134:** 3873–3882.

Wellmer, F., Alves-Ferreira, M., Dubois, A., Riechmann, J.L., and Meyerowitz, E.M. (2006). Genome-wide analysis of gene expression during early *Arabidopsis* flower development. PLoS Genet. **2:** e117.

Wellmer, F., and Riechmann, J.L. (2005). Gene network analysis in plant development by genomic technologies. Int. J. Dev. Biol. **49:** 745–759.

Wellmer, F., Riechmann, J.L., Alves-Ferreira, M., and Meyerowitz, E.M. (2004). Genome-wide analysis of spatial gene expression in *Arabidopsis* flowers. Plant Cell **16:** 1314–1326.

Wu, D., Lim, E., Vaillant, F., Asselin-Labat, M.L., Visvader, J.E., and Smyth, G.K. (2010). ROAST: Rotation gene set tests for complex microarray experiments. Bioinformatics **26:** 2176–2182.

Wuest, S.E., O'Maoileidigh, D.S., Rae, L., Kwasniewska, K., Raganelli, A., Hanczaryk, K., Lohan, A.J., Loftus, B., Graciet, E., and Wellmer, F. (2012). Molecular basis for the specification of floral organs by APETALA3 and PISTILLATA. Proc. Natl. Acad. Sci. USA **109:** 13452–13457.

Wuest, S.E., Vijverberg, K., Schmidt, A., Weiss, M., Gheyselinck, J., Lohr, M., Wellmer, F., Rahnenführer, J., von Mering, C., and Grossniklaus, U. (2010). *Arabidopsis* female gametophyte gene expression map reveals similarities between plant and animal gametes. Curr. Biol. **20:** 506–512.

Yadav, R.K., Girke, T., Pasala, S., Xie, M., and Reddy, G.V. (2009). Gene expression map of the *Arabidopsis* shoot apical meristem stem cell niche. Proc. Natl. Acad. Sci. USA **106:** 4941–4946.

Yanofsky, M.F., Ma, H., Bowman, J.L., Drews, G.N., Feldmann, K.A., and Meyerowitz, E.M. (1990). The protein encoded by the *Arabidopsis* homeotic gene agamous resembles transcription factors. Nature **346:** 35–39.

Yant, L., Mathieu, J., Dinh, T.T., Ott, F., Lanz, C., Wollmann, H., Chen, X., and Schmid, M. (2010). Orchestration of the floral transition and floral development in *Arabidopsis* by the bifunctional transcription factor APETALA2. Plant Cell **22:** 2156–2170.

Yu, H.J., Hogan, P., and Sundaresan, V. (2005). Analysis of the female gametophyte transcriptome of *Arabidopsis* by comparative expression profiling. Plant Physiol. **139:** 1853–1869.

Zheng, X., Zhu, J., Kapoor, A., and Zhu, J.K. (2007). Role of *Arabidopsis* AGO6 in siRNA accumulation, DNA methylation and transcriptional gene silencing. EMBO J. **26:** 1691–1701.